

A mathematical model for the germinal center morphology and affinity maturation

Michael Meyer-Hermann

Institut für Theoretische Physik, TU Dresden, D-01062 Dresden, Germany
E-Mail: meyer-hermann@physik.tu-dresden.de

Abstract: During germinal center reactions the appearance of two specific zones is observed: the dark and the light zone. Up to now, the origin and function of these zones are poorly understood. In the framework of a stochastic and discrete model several possible pathways of zone development during germinal center reactions are investigated. The importance of the zones in the germinal center for affinity maturation, i.e. the process of antibody optimization is discussed.

1 Introduction

Germinal centers (GC) are an important part of the humoral immune response. They develop after the activation of B-cells by antigens. Such activated B-cells migrate into the follicular system where they begin a monoclonal expansion in the environment of follicular dendritic cells (FDC). This phase of pure centroblast multiplication is followed by a phase of intense hypermutation and proliferation which leads to a larger repertoire of different centroblast types. This seems to be the basis of the affinity maturation process, i.e. the optimization process of the antibodies with respect to a given antigen during germinal center reactions. Antigen fragments are presented on the surface of the FDCs which enables antibody presenting cells to interact with them. It is widely believed that centroblasts do not present antibodies (Han *et al.*, 1997). Accordingly, the selection process must begin after the differentiation of centroblasts to centrocytes (the initiation of this differentiation process is still unclear) which do neither proliferate nor mutate but which present antibodies. The centrocytes have initiated a process of apoptosis, so that they have a finite life time (Liu *et al.*, 1989; Liu *et al.*, 1994). They have to be rescued from apoptosis through an interaction with the antigen fragments on the FDCs and with T-helper cells (Brandtzaeg, 1996; Tew *et al.*, 1997; Hollmann & Gerdes, 1999; Hur *et al.*, 2000; Eijk *et al.*, 2001). This at least two step selection process (Lindhout *et al.*, 1997) primarily depends on the affinity of the tested antibody and the antigen. Therefore, the affinity maturation during GC reactions rests on two major pillars: the hypermutation of centroblasts and the affinity dependent antigen-specific selection of centrocytes.

The morphology of the GCs is very specific and shows properties which are characteristic for different stages of the reaction (Liu *et al.*, 1991; Camacho *et al.*, 1998). In a first stage – the phase of monoclonal expansion – a system of FDCs is continuously filled with proliferating centroblasts. Then the centroblasts begin to differentiate into centrocytes and the selection process begins. In this second phase the two types of B-cells, centroblasts and centrocytes, form two zones (Nossal, 1991): the dark zone which is dominated by proliferating and hypermutating centroblasts, and the light zone containing centrocytes and FDCs. These two zones are stable for at least some days and may then disappear. In the third morphological phase the centroblasts and centrocytes are homogeneously distributed over the GC (Camacho *et al.*, 1998). The number of cells is now continuously declining until the end of the GC reaction. The total GC life time is about 21 days (Jacob *et al.*, 1991; Liu *et al.*, 1991; Kelsoe, 1996).

Up to now, the role and the reason for the appearance of the dark and the light zone have not been resolved. These problems are here investigated in the framework of a stochastic 2+1-dimensional space-time model. Until now, only dynamical models for the GC reaction without resolution of spatial aspects have been developed (Oprea & Perelson, 1996, 1997; Rundell *et al.*, 1998; Kesmir & de Boer, 1999; Oprea *et al.*, 2000; Meyer-Hermann *et al.*, 2001). However, for the analysis of the GC zones this is essential. In the present article several possible dynamic pathways and requirements for the development of dark and light

zones are discussed. The stability of the zones, i.e. the duration of centroblast-centrocyte separation, and their role within the affinity maturation process are analysed.

It is very important to carefully analyse the existing experimental knowledge. Therefore, the discussion of the model assumptions (see Sec. 2) will frequently refer to the experimental situation, and the model parameters will be determined directly or indirectly using corresponding data. The section on the model development is divided into three parts: A short review of the shape space concept for the representation of antibody types (Sec. 2.1), a discussion of the dynamical properties of the GC during different stages of the reaction (Sec. 2.2), and the introduction of the spatial aspects, i.e. cell movements and cell interactions (Sec. 2.3). Naturally, these subsections are interlinked, so that some repetition is unavoidable. The dynamical properties and the local cell interactions lean upon a deterministic model developed before (Meyer-Hermann *et al.*, 2001). A presentation of the results follows in Sec. 3 including a discussion of necessary and sufficient requirements for the development of dark zones (Sec. 3.1), of the implications of dark zones for affinity maturation (Sec. 3.3 and 3.4), and of the robustness of the results with respect to different physiological quantities entering the model (Sec. 3.6). Finally, the results are summarized and evaluated (Sec. 4).

2 Model development

A model describing morphological properties of the GC reaction needs to have three basic aspects: the representation of antibodies, the dynamics and the interaction between the cells, and their spatial distribution. These aspects already define the structure of this section. It is worth emphasizing that this section is not only devoted to the formulation of postulates, but also to give an experimental motivation for the assumptions and to determine the physiological quantities which enter the model. A careful discussion of the physiological parameters builds the fundament of the model stability and of its relation to real GCs. The resulting parameter values are summarized in Table 1.

2.1 Representation of antibody and antigen phenotype

In order to describe the affinity maturation process during GC reactions, the antibodies encoded by B-cells as well as antigens are represented with the help of the shape space concept (Perelson & Oster, 1979). A D -dimensional finite size lattice is defined in which each point corresponds to one antibody phenotype (accordingly, the shape space does not provide a representation of the genetic variability of antibodies). A phenotypically relevant mutation is represented by a jump to a nearest-neighbor point in the shape space, which means that a single mutation of the B-cell does not lead to a random change of the antibody phenotype.

The antigen is represented in the same shape space using the assumption of optimal complementarity, i.e. it exists a corresponding type of antibody having a maximal affinity.

The antigen is represented by the point in the shape space, which corresponds to this optimal antibody.

The representation of mutations by jumps to neighbor points in the shape space allows the affinity of antibodies of mutating B-cells to be enhanced successively, which is believed to happen during GC reactions. This property may be called *affinity neighborhood* and means that antibodies on neighboring points in the shape space do not have drastically different affinities with respect to a given antigen. The relevance of possibly existing key mutations that imply considerable changes of the affinity was discussed before (see Meyer-Hermann *et al.*, 2001).

This concept allows a quantitative formulation of a smooth affinity function on the shape space, describing the affinity of a given antibody to a given antigen. Denoting the antibody type and the antigen by the shape space points ϕ and ϕ^* , respectively, one can define the affinity weight function

$$a(\phi, \phi^*) = \exp\left(-\frac{\|\phi - \phi^*\|^\eta}{\Gamma^\eta}\right), \quad (1)$$

where $\Gamma \approx 2.8$ is the width of the affinity weight function, $\|\cdot\|$ denotes the Euclidean metric, and $\eta = 2$ is the exponent of the distance in the shape space. These values were determined from existing data of affinity enhancement in dependence on the number of observed mutations (for details see Meyer-Hermann *et al.*, 2001, Fig. 2).

In a physiological GC reaction we do not only expect to find different antigen fragments but also different antigens. Nevertheless, in experiments the immunization is often performed by the injection of one specific antigen. Therefore, in the present model we assume only one antigen to be present during the GC reaction. However, it may be interesting to investigate the dynamical changes of GC reaction with more than one antigen.

2.2 Germinal center phases

There exist many different pictures describing the stages of a GC reaction, both from the perspective of dynamical interactions and of morphological properties. Here, a rather general point of view is adopted which is based on widely accepted observations and interpretations of the GC. We hope that this enhances the validity of the model implications.

The whole GC reaction is initiated by the migration of antigen-activated B-cells into the follicle system. The model description starts when the activated B-cells are present in the environment of antigen presenting FDCs in the follicle system. The affinity of these cells to the antigen is assumed to be low but non-vanishing (as they were activated). In the model this is represented by a typical distance of the B-cells from the antigen in the shape space between 5 and 10, i.e. the B-cells have to hypermutate at least 5 times in order to find the optimal antibody type with respect to the antigen. This number is in accordance with the one observed in experiment (Küppers *et al.*, 1993; Wedemayer *et al.*, 1997). Note that here only the hypermutations of phenotypical relevance are counted.

2.2.1 The phase of monoclonal expansion

The activated B-cells (centroblasts) start to multiply in the presence of the FDCs. This process of intense expansion – the proliferation rate is about $1/(6hr)$ (Hanna, 1964; Zhang *et al.*, 1988; Liu *et al.*, 1991) – is believed to be monoclonal (Jacob *et al.*, 1993; McHeyzer-Williams *et al.*, 1993; Pascual *et al.*, 1994a; Han *et al.*, 1995a), so that no somatic hypermutations occur in this stage of the GC reaction, and the antibody type encoded by the centroblasts remains unchanged. Furthermore, the expanding centroblasts do not seem to present antibodies on their surface (Han *et al.*, 1997) – at least in this first phase (this has recently been questioned (Berek, 2001)). As a consequence, in the model no interaction with antigen fragments or T-helper cells is provided during this phase.

GCs develop oligoclonally (Kroese *et al.*, 1987; Liu *et al.*, 1991; Jacob *et al.*, 1991; Küppers *et al.*, 1993), i.e. the number of initial centroblasts is small. It has been shown that after three days of centroblast expansion all B-cells in average stem from about three to six seeder cells. Within three days (this is the duration of this first phase (Liu *et al.*, 1991)) the FDC network is completely filled with centroblasts (Camacho *et al.*, 1998). The volume occupied by centroblasts even exceeds the FDC network. The total number of centroblasts reaches about 12000 cells in this stage of the reaction.

2.2.2 Early optimization phase

The phase of B-cell selection by interaction of antibody presenting centrocytes with antigen fragments on the FDCs is characterized by the following additional dynamical properties:

Somatic hypermutation The centroblasts continue to proliferate at the same rate. Additionally, they have a high probability of somatic hypermutations of $m = 0.5$ (Berek & Milstein, 1987; Nossal, 1991) leading to a higher variability of antibody types in the GC. This property provides the basis of the affinity maturation process and is incorporated into the model by a random probability of $m = 0.5$ for each dividing centroblast to switch to a randomly chosen neighbor point in the shape space. Consequently, in average one of the two new centroblasts emerging from a cell division will correspond to a changed antibody.

Differentiation to centrocytes The centroblasts differentiate into centrocytes (Liu *et al.*, 1991; MacLennan, 1994; Choe *et al.*, 2000). The initiation of this differentiation process is still unclear. One may suspect a centroblast differentiation after a fixed lifetime or an unknown signal of unknown provenience. Several options for the initiation of the differentiation process will be discussed in the framework of the model. The process itself is assumed to take some time, i.e. a centroblast in the state of differentiation will become a centrocyte with a rate g_1 . This rate determines the speed of the whole GC reaction (Meyer-Hermann, 2001) and has been observed in experiment. At a certain stage of the GC reaction the proliferating cells were labeled and it was found that after 7 hours these cells were present in the light zone in a non-proliferating stage (Liu *et al.*, 1991; Berek,

2001), i.e. they differentiated to centrocytes and moved into the light zone within 7 hours. Therefore, the differentiation rate has to be slightly larger than $1/(7hr)$. On the other hand, it should not differ drastically from the proliferation rate as otherwise the total cell population would either die out or explode on a small time scale (Meyer-Hermann, 2001). Taking these arguments together one is led to a centroblast to centrocyte differentiation rate of approximately $g_1 = 1/(6hr)$.

Apoptosis of centrocytes Unbound centrocytes have initiated an apoptotic process. If apoptosis is not suppressed in time the centrocytes will die. The typical life time of centrocytes has been estimated to be 6 to 16 hours (Liu *et al.*, 1994). Correspondingly, the rate of centrocyte death z is chosen in this range. A value of $z = 1/(7hr)$ turns out to be most advantageous for the affinity maturation. Dead cells are rapidly engulfed by macrophages so that in the model they are removed from the lattice rapidly. The speed of this process has a marginal impact on the space available for the movement of the remaining cells.

Centrocyte-FDC-interaction As the GC contains more and more centrocytes due to the centroblast differentiation process during this phase, the interaction of the presented antibodies with the antigen fragments on the FDCs has to be taken into consideration. The inhibition of centrocyte apoptosis is believed to depend on this interaction process as well as on the interaction with T-helper cells (Lindhout *et al.*, 1995; Brandtzaeg, 1996; Tew *et al.*, 1997; Hollmann & Gerdes, 1999; Hur *et al.*, 2000; van Eijk *et al.*, 2001). Conversely, also the acceleration of apoptosis of non-binding centrocytes has been discussed (Hollmann & Gerdes, 1999). In the framework of such regulation processes, the role of CD40-CD40L-interaction, Fas-FasL-interaction, and bcl-2-expression are currently under investigation (Han *et al.*, 1997; Choe & Choi, 1998; Choe *et al.*, 2000; van Eijk *et al.*, 2001; Siepmann *et al.*, 2001). We do not propose a solution to this puzzle in the model, but we effectively incorporate the inhibition of apoptosis.

In order to allow affinity maturation the interaction of centrocytes with FDCs is assumed to depend on the affinity of antibody and antigen (Liu *et al.*, 1989; Koopman *et al.*, 1997; Radmacher *et al.*, 1998). In the model this is represented by the affinity weight function Eq. (1): Each time a centrocyte is in local contact with an FDC, i.e. they are direct neighbors on the spatial lattice, it will bind to the antigen with a probability $a(\phi, \phi^*)$ that is given by the affinity of the antibody presented by the centrocyte to the antigen fragment presented by the FDC. An effective binding rate for centrocytes and FDCs is implicitly introduced using corresponding rules for the interaction (see Sec. 2.3.1 *Centrocytes*). This binding rate basically depends on the centrocyte diffusion constant D_{CC} and on the cell distribution around the centrocyte.

Once a centrocyte is bound, it remains bound to the FDC for a certain time. The above mentioned rescue processes are thought to take place during this time. Unfortunately, the duration of binding is not known experimentally. However, the observation that the process

of apoptosis of a centrocyte is stopped within 2 hours (Lindhout *et al.*, 1995; van Eijk & de Groot, 1999) may provide a valuable hint: Assuming that the inhibition of apoptosis is done during the binding of centrocyte and FDC and that the centrocytes dissociate from the FDC afterwards, the rate of centrocyte-FDC dissociation becomes $g_2 = 1/(2hr)$.

Recycling of centrocytes Positively selected centrocytes, i.e. B-cells encoding antibodies of high affinity to the antigen, may reenter the state of proliferation and mutation. This possibility is the frequently discussed recycling hypothesis (Kepler & Perelson, 1993; Han *et al.*, 1995a; Oprea *et al.*, 2000; Meyer-Hermann *et al.*, 2001), which has not been proven in experiment until today. It has to be clarified what is explicitly meant by recycling. In some definitions of the recycling process the recycled cells do not only restart to proliferate and to mutate but also return to the dark zone (Kelsoe, 1996; Han *et al.*, 1997). In the present model a more modest variant is adopted, i.e. recycling solely denotes the possibility of reentering the state of proliferation and mutation – independently of where this happens and where these cells tend to go. Therefore, our model does not exclude proliferating cells in the light zone, and it will be discussed if a reentry into the dark zone is possible or even necessary.

Differentiation into plasma- and memory-cells During the phase of early optimization no production of plasma- and memory-cells is provided by the model (see Sec. 2.2.3), i.e. all positively selected centrocytes are recycled.

Signal molecules All processes described so far are based on the production of signal molecules which lead to a *local* interaction between the cells, i.e. each signal is related to an interaction with a very specific B-cell. This especially is the case for the inhibition of apoptosis in positively selected centrocytes as well as for the differentiation path of rescued B-cells (into plasma- or memory-cells or back into a stage of proliferation). Such local interaction processes are assumed to be necessary for affinity maturation, as it is difficult to imagine a non-local interaction rescuing specific B-cells of high affinity to the antigen. Therefore, we assume in our model that these interactions take place during the binding of centrocytes to FDCs. For this reason no signal molecule has to be specified explicitly, since it is completely sufficient to incorporate the corresponding functional answer of the cells into the model.

Nevertheless, one should be aware that the centrocytes take the antigen fragments with them, i.e. B-cells that have successfully interacted with the FDCs are recognizable in this way. Therefore, a non-local interaction with a diffusing signal molecule (which may be secreted for example by the FDCs) which targets specific B-cells with bound antigen fragments may exist. Such a specific non-local interaction may be in accordance with affinity maturation if a mechanism is utilized which recognizes B-cells transporting antigen fragments. This case is not covered by the model assumption of local interactions. However, the efficiency of such a non-local interaction process would be smaller compared

to a local interaction: If a high affinity B-cell is detected at the FDCs, this information is lost through its dissociation from the FDC, and the same cell must be detected for a second time by signal molecules. This is an unreasonable procedure, especially for the inhibition of apoptosis which is a time critical process.

The situation is different for the differentiation of centroblasts to centrocytes. Adopting the reasonable assumption that all centroblasts will differentiate into centrocytes independently of their affinity to the antigen there exists no obvious reason for a local interaction. On the other hand, the presence of FDCs and T-cells is believed to be important for the differentiation process of centroblasts (Dubois *et al.*, 1999a, 1999b; Choe *et al.*, 2000). So if FDCs or T-cells trigger the differentiation of centroblasts but not by a local interaction with single B-cells, a non-local interaction becomes obligatory. In order to allow a non-local interaction in the model we incorporate a diffusing signal molecule (see Sec. 2.3.1) which triggers the centroblast differentiation, is produced by the FDCs, and is bound by the centroblasts. This feature should not be considered an assumption but an option of the model. Alternative pathways of differentiation will be discussed.

2.2.3 The phase of late optimization and output production

The duration of the early optimization phase Δt_2 determines the starting point of the phase of late optimization and output production, which differs from the early optimization phase solely by an additional pathway of differentiation for positively selected centrocytes. It is widely believed that the interaction between centrocytes and FDCs may involve a local differentiation signal which enables the centrocytes to further differentiate into plasma or memory cells (shortly denoted as *output cells* in the following) or – as discussed before – back into a proliferating B-cell state.

A delay Δt_2 in the production of plasma- and memory-cells with respect to the start of hypermutations was indeed observed experimentally (Jacob *et al.*, 1993; Pascual *et al.*, 1994b) and is of the order of 48 hours. This justifies the separation of optimization and output production phase in the model. In addition it has previously been shown that such a delay is necessary in order to get an appropriate average quality of produced output cells. This delay could be determined quantitatively using the experimental observation that the number of produced output cells multiplies by a factor of 6 between day 6 and day 12 after immunization (Han *et al.*, 1995b). The steepness of the number of produced output cells versus time is directly influenced by the duration of the optimization phase. In this way one is led to a delay of the output production phase of 48 hours (Meyer-Hermann *et al.*, 2001), which is in perfect accordance with the above mentioned experimental observation. Therefore, this value is assumed for the present model and the resulting steepness of the output production will be verified subsequently (see Sec. 3.2). Nevertheless, it would be interesting to discuss possible mechanisms which may generate the start of output production dynamically.

Positively selected centrocytes differentiate into output cells at a rate of $g_3 = 1/(7 \text{ hr})$. As we assumed recycling to exist, the proportion of differentiation into output cells to

differentiation into a re-proliferating cell state has to be chosen. The recycling probability of positively selected B-cells is determined by the only known experimental evidence for recycling (Han *et al.*, 1995a). A quantitative evaluation (Meyer-Hermann *et al.*, 2001) leads to a probability of $q = 80\%$, i.e. 4 out of 5 positively selected B-cells do not differentiate into plasma- or memory-cells but restart to proliferate and mutate, and only one cell differentiates into an output-cell.

2.2.4 The end of the GC reaction

The whole GC reaction lasts about 21 days (Jacob *et al.*, 1991; Liu *et al.*, 1991; Kelsoe, 1996). No consumption of antigen fragments (Tew & Mandel, 1979) is postulated and no production of antibodies by plasma cells is assumed in order to stop the GC reaction. The model assumes that the main course of the cell population dynamics is governed by the local cell interactions and thus is independent of antigen consumption (Meyer-Hermann *et al.*, 2001). As the amount of presented antigen is reduced to 50% during 30 days (Oprea *et al.*, 2000), i.e. during the whole GC life time, it is unlikely that the fast reduction of the total cell population after about 5 days (Liu *et al.*, 1991; Hollowood & Macartney 1992) is due to antigen consumption.

Note, that if plasma cells differentiate inside the GC they may also produce antibodies there. These antibodies could bind the antigen fragments and in this way reduce the probability of selection of centrocytes if a large number of antibodies is present inside the GC. This effect may become important at the end of the GC reaction, when the number of plasma cells has already increased. The final phase of the GC would be shortened compared to the model results. The resulting final state of the GC reaction as it appears in this model will be further discussed (see Sec. 3.5).

2.3 Spatial distribution on a lattice

One major task of the model is to find possible explanations for the specific morphological appearance of GCs. Especially, the dark and light zones are of interest, as it remains unclear if they may be or why they are essential for affinity maturation. A deeper understanding of these connections may be important in view of malignant GCs as well (Falini *et al.*, 2000; Dunn-Walters *et al.*, 2001).

The spatial distribution of the B-cells and FDCs is implemented in an equidistant lattice of fixed volume. This constant volume is considered as reaction volume and thus is not identical to the real GC volume. The latter is defined by the volume occupied by all B-cells in the reaction volume and will consequently change in time. The resulting GC volume time course is compared to experimental data from real GC reactions in Sec. 3.5. Note, that in this prescription possible changes of the GC dynamical behavior due to the interaction with naive B-cells in the mantle zone, for example, are neglected.

Each lattice point can contain one cell only. Signal molecules can accumulate at every lattice point. The cell movement is basically governed by diffusion (see Sec. 2.3.4). The

lattice constant is chosen to correspond to a typical B-cell diameter. Centroblasts have a radius of about $r_{CB} \approx 7.5 \mu m$ (Kroese *et al.*, 1987; Hostager *et al.*, 2000) and centrocytes are substantially smaller (Liu *et al.*, 1994). The average radius is of the order of $5 \mu m$, and we are led to a lattice constant of $\Delta x = 10 \mu m$. However, this value solely has an influence on the cell mobility and therefore is not an independent parameter of the model but determines the meaning of the diffusion constants (see Sec. 2.3.4).

2.3.1 B-cell, FDC, and signal representation

In the following the specific treatment of the different cell types on the lattice and the corresponding actions are explained in terms of rules for cell behavior. In principle, every cell is characterized by its position on the lattice, the state of differentiation, and the type of encoded antibody in the shape space (see Sec. 2.1). Note that not all possible actions will occur in all phases of the GC reaction (see Sec. 2.2). Note further that in general some actions are forbidden to occur in the same time step. This is no relevant restriction if the time steps are sufficiently small, so that in most time steps no action occurs at all.

Centroblasts can be in two different states: Originally, an *unsignaled* centroblast can proliferate, mutate, and diffuse. When it meets a threshold concentration of the differentiation signal it switches to the state *signaled* and can additionally differentiate into centrocytes (with rate g_1).

At each time step the concentration of signal molecules is checked at the same lattice point. The state of the centroblast is chosen correspondingly. In any case the B-cell remains a centroblast. It then tries to proliferate (see Sec. 2.3.3) and, provided that it is in the state *signaled*, tries to differentiate into centrocytes (with rate g_1). Only one of the last two actions is allowed and both actions are tried in a random sequence. If the centroblast proliferates both new centroblasts mutate (change the position in the shape space) with probability m . If the centroblast did not differentiate to a centrocyte it might also diffuse with diffusion constant D_{CB} . A diffusion beyond the GC volume is forbidden.

Centrocytes emerge through differentiation of centroblasts only. They can be in three different states: First they are *unselected*, may then get in *contact* with FDCs, and finally may become positively *selected*.

- An unselected centrocyte dies with a rate z . A dead centrocyte is eliminated from the lattice.
- During its life time it checks for an FDC on the neighbor lattice points. If there is one, the switch to the state *contact* is weighted with the affinity function Eq. 1. A centrocyte which has tried in vain to get into contact with an FDC has to move by diffusion before it may try again (this introduces an absolute time scale for the binding process which is basically determined by the centrocyte diffusion constant D_{CC}).

- A centrocyte in contact with an FDC dissociates from it and switches to the state *selected* with rate g_2 . It can neither move nor die.
- A positively selected centrocyte further differentiates with rate g_3 into an output cell with probability $1 - q$ or a centroblast with probability q . If the centrocyte did not differentiate it might diffuse with diffusion constant D_{CC} .
- The diffusion of centrocytes beyond the GC volume is forbidden independently of its state.

Output cells diffuse on the lattice with diffusion constant D_{CC} . They have no restriction at the border of the GC volume, i.e. if an output cell diffuses beyond the GC volume it is eliminated from the lattice. An eliminated output cell is memoried and contributes to the total (i.e. time integrated) output production.

FDCs are represented on the lattice by a center with $2d$ arms of $30 \mu m$ length, where d is the space dimension of the lattice. These cells are assumed to be immobile. This does not correspond to reality as at least the arms of the FDCs are steadily looking for an interaction partner. However, this is not an important restriction, since the movement of the FDCs would primarily change the interaction frequency of FDCs and centrocytes, which may be achieved by a faster centrocyte diffusion as well.

The differentiation signal is represented as a discretized density on the whole lattice. One quantum of the signal is thought to contain exactly as many molecules as are necessary to induce the differentiation process in one centroblast. Those quanta move on the lattice according to a classical diffusion equation (see Sec. 2.3.4) independently of the cell distribution on the lattice. In order to keep the quanta undivided, the movement of the remaining non-integer part of a quantum is chosen randomly in each time step. If an unsigned centroblast is present on the same lattice point at some time step, one of those quanta at this point is eliminated from the lattice and the state of the centroblast is changed to *signaled*. The signal molecules may diffuse beyond the GC volume. In this case they are eliminated from the lattice.

2.3.2 Initial cell distribution

At the beginning of the GC reaction only FDCs and a few seeder cells (centroblasts) are present in the follicle system. The follicular network is completely filled during the phase of monoclonal expansion (Liu *et al.*, 1991; Camacho *et al.*, 1998). The centroblasts even need slightly more space than provided by the FDC network. This is incorporated into the model by a random initial distribution of the FDC on a lattice area which is restricted to about 70% of the maximal GC volume. However, for reasons of clarity and of comparability of the results, all simulations presented in this article are based on the same

FDC distribution (see Sec. 3.6.1). The number of seeder cells is chosen to be 3 (Kroese *et al.*, 1987; Liu *et al.*, 1991; Jacob *et al.*, 1991; Küppers *et al.*, 1993). They are randomly distributed on the FDC network.

2.3.3 Spatial aspects of proliferation

The proliferation process itself is not only dependent on the proliferation rate but also on the environment of the dividing centroblast. Principally, a centroblast can only proliferate if there is a free lattice point in its neighborhood. On the other hand, this scenario is not realistic, as the centroblasts may deform and the dividing process does conserve the total volume of both new cells. A strong exclusion rule that forbids proliferation if all neighbor points are occupied would therefore strongly decrease the number of proliferations compared to a realistic or exponential increase of the total cell number. The solution we propose is to allow the proliferation if there is a free lattice point within a sphere around the dividing cell. The centroblasts in the environment of the dividing cell are rearranged in such a way that the proliferation becomes possible. In this picture a dividing cell is able to push away a maximal number of cells which corresponds to the radius R_P of this theoretical sphere. Within the sphere the centroblasts expand exponentially. When the centroblasts expand beyond our theoretical sphere a nucleus of centroblasts, which are no longer able to proliferate until the surrounding cells are spread through diffusion, emerges, and the exponential growth is slowed down. Therefore, the resulting total number of centroblasts is directly changed in dependence on the sphere radius. As the number of centroblasts after 3 days of the GC reaction is known experimentally, the radius is chosen correspondingly, where a value of $R_P = 60 \mu m$ appears to be reasonable. This spatial proliferation model has realistic features which are sufficient for our purpose as we are not primarily interested in the details of the proliferation process. Nevertheless, a more detailed mechanistic model may lead to new dynamical insights (Beyer & Meyer-Hermann, 2002).

2.3.4 Movement of cells and molecules

Centroblasts, centrocytes, and signal molecules essentially move by diffusion. This is realized on the lattice by a probability of moving to a free neighbor point on the lattice which can be calculated using the classical diffusion equation

$$\frac{\partial c}{\partial t} = D \sum_{i=1}^d \frac{\partial^2 c}{\partial x_i^2} \quad , \quad (2)$$

where c is the population of the diffusing cell type, d denotes the dimension of the lattice, t the time, and x_i the spatial coordinates. This equation is translated to a discrete equation with lattice constant $\Delta x = \Delta x_i$ (the lattice is equidistant) and time step Δt

$$\frac{\Delta c}{\Delta t} = D \sum_{i=1}^d \frac{\Delta^2 c}{\Delta x^2} = D \frac{-N}{\Delta x^2} \quad , \quad (3)$$

where N is the number of free neighbor points that can adopt values between 0 and $2d$. Using this one may define a statistical probability p_{diff} for one cell to move to a free neighbor point:

$$p_{\text{diff}} = D N \frac{\Delta t}{\Delta x^2} . \quad (4)$$

One should be aware that this probability is based on the assumption that each lattice point can be occupied by one cell only. Therefore, the diffusion of signal molecules, which do not undergo this restriction, has to be treated according to the more general first part of Eq. (3).

It is worth emphasizing that the assumption to allow only one centroblast or centrocyte at each lattice point, independently of the volume occupied by these cells, does not imply the neglect of the differing cell diameters. The cell volume primarily has an impact on the mobility of the cells. Therefore, the cell diameters are incorporated into the model by using different diffusion constants D_{CB} and D_{CC} for centroblasts and centrocytes, respectively. Quantitatively, the relation between both parameters is determined by the relation between the diameters: Considering the cells as spheres of a specific radius r moving in a medium of viscosity η at temperature T under influence of friction according to Stokes, the diffusion constant becomes

$$D = \frac{kT}{6\pi\eta r} , \quad (5)$$

where $k = 1.3806610^{-23} J/K$ is the Boltzmann constant. At room temperature $T = 293 K$, with a viscosity for blood of $\eta = 0.02 Js/m^3$ (Skalak & Chien, 1987), and with a cell radius of $2.5 \mu m$ and $7.5 \mu m$ for centrocytes and centroblasts, respectively, (Kroese *et al.*, 1987) (see also Liu *et al.*, 1994 for the ratio of both radii) one finds

$$D_{\text{CB}} \approx 5 \frac{\mu m^2}{hr} ; \quad D_{\text{CC}} \approx 15 \frac{\mu m^2}{hr} . \quad (6)$$

Surely, the absolute values of these diffusion constants have been estimated very roughly. Especially, the lymphocytes do not diffuse in blood but in lymphoid organs. Additionally, the movement of the FDCs effectively increases the observed diffusion constant in the model. Finally, the assumption of a friction according to Stokes may be questioned. Nevertheless, the assumption that the diffusion constants depend on the cell radii is reasonable, and the ratio of the radii is relatively sure. Therefore, the main uncertainty concerns the absolute values of the diffusion constants, not their ratio (see Sec. 3.6.4).

The diffusion of signal molecules is assumed to be considerably faster than the diffusion of the cells, with the diffusion constant being of the order of (Murray, 1993)

$$D_{\text{Sig}} \approx 200 \frac{\mu m^2}{hr} . \quad (7)$$

2.3.5 A two-dimensional projection

In order to compare the model results with pictures of slices containing GCs, the model is realized on a two-dimensional (2D) lattice. One should be aware that a three-dimensional

(3D) model may open new pathways for cell movements, so that a more realistic three-dimensional model may lead to different dynamical properties in some aspects. Nevertheless, we expect the basic properties to remain untouched from this projection on a two-dimensional lattice. The comparison of the results in a 2D and a 3D model is the task of a separate work.

It is important to project the physiological parameters on the 2D lattice. This concerns all parameters which have an impact on the spatial distribution of the cells in the GC, i.e. the proliferation rate, which controls the creation of new cells at specific positions, the number and the geometry of the FDCs, and the total volume of the GC. The diffusion constants are defined for an arbitrary lattice dimension (see above) and the diameters of the spheric cells remain unchanged in a two dimensional plane.

Proliferation rate The proliferation rate in a 3D-GC of $1/(6hr)$ corresponds to $1/(9hr)$ in a 2D lattice, as only 4 of 6 new cells emerging from a proliferation process will appear in the 2D plane. Therefore, the final number of B-cells after 3 days of monoclonal expansion will not be 12288 as in an idealized 3D model but 768.

GC-volume The maximal number of cells determines the total size of the 2D lattice. According to experimental observations (Liu *et al.*, 1991; Camacho *et al.*, 1998) the FDC network, i.e. the volume of the GC is completely filled with centroblasts after 3 days of proliferation. Starting from a typical GC volume three days after immunization of 0.05 mm^3 , we end up with a GC radius of $232\text{ }\mu\text{m}$ or 47 lattice points per dimension. Based on this rough estimate, the number of lattice points per dimension is fixed to 45 corresponding to a radius of $220\text{ }\mu\text{m}$. This still allows a certain cell movement even if the cell number in the GC is at its maximum.

FDCs The number of arms of the FDCs is reduced from 6 (3D) to 4 in the 2D model. The length of the FDC arms remains unchanged. It is worth emphasizing that the FDC arm length and the number of FDCs together determine the available surface for interaction with centrocytes, and in this way influence the interaction frequency of centrocytes and FDCs. The total number of FDCs is chosen in such a way that the centrocytes have enough space to move and at the same time have enough possibilities to interact with FDCs, i.e. the number of binding sites on the FDCs should be of the order of the maximal number of centrocytes. As centrocytes differentiate from centroblasts and the centroblast differentiation rate is of the same order as the centrocyte apoptosis rate, the maximal number of centrocytes will lie roughly in the same range as the maximal number of centroblasts. For an FDC arm length of $30\text{ }\mu\text{m}$ this leads to about 20 FDCs in a 2D-GC with a radius of $220\text{ }\mu\text{m}$.

3 Results

The previous section was devoted to the physiological motivation of model assumptions and to the determination of the model parameters by experimental data. In the present section the results of the numerical realization of this stochastic model will be presented. As in some cases the experimental constraints for the physiological quantities were not strong enough, there still remains a certain freedom of choice for some of them. Therefore, these quantities will have to be optimized iteratively with respect to the outcome within their physiological range. The parameters in Tab. 1 turned out to be an optimal choice with respect to different aspects of the GC reaction, which will be described below.

However, the presentation of the results will not start from these optimal values, since the necessity of some model assumptions is better illustrated by going through the different stages of the model development. Therefore, the discussion starts with the consideration of different scenarios for the establishment of the dark zone during GC reactions (see Sec. 3.1). Based on the results of this subsection a reference GC is defined (see Sec. 3.2). Afterwards, it is discussed how the duration of the dark zone is determined (see Sec. 3.3), and the influence of B-cell recycling and the dark zone on the optimization process, i.e. on affinity maturation, is investigated (see Sec. 3.4). Finally, we discuss the evolution of the total GC volume (see Sec. 3.5).

3.1 Requirements for dark zones

FDC inhomogeneity An important task of this work is to investigate necessary and sufficient conditions for the emergence of a dark zone during GC reactions. The seed of a dark zone appears to be an inhomogeneity of the FDC distribution on the GC volume. During the first phase of the reaction the initial centroblasts proliferate beside and/or inside the FDC network. However, at least some of the centroblasts proliferate outside the FDC network or expand beyond it. It is exactly these centroblasts that give rise to the development of the dark zone. As in the model the maximal GC volume (i.e. the lattice volume) is fixed a priori, this dynamical behavior is simulated by a statistical distribution of the FDCs on a restricted area of the GC which occupies about 70% of the total GC volume. Without such a restricted distribution of the FDCs the distribution of centroblasts and centrocytes on the GC necessarily becomes homogeneous. Accordingly, the expansion of centroblasts beyond or beside the FDC network is a necessary condition for the development of dark zones, and is independent of the mechanism which is assumed for the initiation of centroblast differentiation into centrocytes. In this perspective, centroblasts, which primarily proliferate outside the FDC network (Camacho et al., 1998), would facilitate the emergence of a dark zone. In the following we start from the more modest point of view, that only a part of the centroblasts is present outside the FDC network after 3 days of proliferation.

Centroblast specific differentiation As will be shown in the following, the centroblast differentiation process is a key element in the development of the dark zone. In a first step we do not investigate any interaction of FDCs with centroblasts or any signal molecules that trigger the differentiation of centroblasts to centrocytes. One may imagine for example the centroblasts to have an internal clock which lets them differentiate after some more or less fixed time. Alternatively, a fixed number of proliferation rounds for each centroblast may be supposed. In both scenarios the differentiation should merely start after three days of monoclonal centroblast expansion, as centrocytes are not present in GCs before this time. This type of hypothesis was tested in the present model and the expected result was found: No dark zone appears at all at any moment of the reaction. This can easily be understood, as the differentiation process is started everywhere in the GC volume at the same time. The differentiating centroblasts are distributed homogeneously, especially in an area which has the potential of becoming the dark zone, i.e. an area without FDCs. This process ends up with a homogeneous distribution of centroblasts and centrocytes over the whole GC volume.

As a consequence, in the framework of the above scenarios the appearance of dark zones is necessarily coupled to an additional force, driving the separation of centroblasts and centrocytes. One may investigate mechanical forces in this context, since both cell types differ in size. This has an impact on their diffusion constant. The radii differ by a factor of at least 2 (Liu *et al.*, 1994), so that the distance the cells may overcome by random walk differs by a factor of about 1.4. Apparently, there exists a slight difference in the mobility of both cell types, but without definite direction. The separation of both cell types may be achieved either by a local attractor for one cell type or by a homogeneous force field. The latter possibility corresponds to the problem of sorting large and small balls in the field of gravity and is presently under investigation (Beyer & Meyer-Hermann, 2002). This possibility cannot be excluded here, even if the origin of such a force field remains unclear from the physiological point of view. At first sight, the existence of a local attractor seems to be a promising assumption as the FDCs may bind only centrocytes but no centroblasts. We tested how long this centrocyte-FDC binding process has to endure in order to get a realistic separation of centrocytes and centroblasts. Unfortunately, no dark zone appears at all (see Fig. 1), even using extremely long centrocyte-FDC interaction times of about 100 *hr*, which is completely unreasonable as in experiment the binding time is estimated to be of the order of 2 *hr* (Lindhout *et al.*, 1995; van Eijk & de Groot, 1999). The reason is that the centroblast differentiation occurs independently of the position in the GC, i.e. homogeneously distributed. Even if there was an increased amount of centroblasts in the area without FDCs, this tendency to a dark zone would be destroyed in the same moment due to the centroblast differentiation process, which takes place everywhere in the dark zone. Therefore, in this scenario one cannot expect to get stable dark zones. They could at the best appear as statistical fluctuations of the centroblast population.

Local centroblast-FDC interaction Now let us turn to a third scenario, where the FDCs initiate the centroblast differentiation by a local interaction. In this case only those centroblasts which are placed at the surface of an already established dark zone would differentiate into centrocytes and the nucleus of the dark zone would remain unaffected by the differentiation at the surface. Therefore, a stable establishment of a dark zone is possible in this scenario. This gives rise to two important questions: How long does a dark zone exist? How does the GC reaction stop? Both questions are answered very clearly by the model and the answers are stable against variations of the model parameters: The dark zone develops early and remains present until the end of the reaction. The total cell population in the GC does not decline but approaches a constant. The FDCs are surrounded by centrocytes which are in selection process, so that spots of FDCs with centrocytes appear on a background of centroblasts (see Fig. 2). The fraction of centrocytes in the FDC network is governed by the selection rates and the FDC density: For large centroblast- and large (selected) centrocyte-differentiation rates and for large FDC densities the fraction of centrocytes can be increased. But the qualitative appearance of the GC does not change. This spot-like GC is not in agreement with experimentally observed GCs. Those have no spots and after a while one finds more centrocytes than centroblasts. In addition, the GC reaction declines after 3 weeks. In the model a reduction of the total cell population can only be achieved by an additional assumption concerning the proliferation rate. Taking into account that the dark zone has been observed to disappear after 8 days (Camacho *et al.*, 1998) and that the total GC volume already decreases at day 5 (Liu *et al.*, 1991; Hollowood & Macartney 1992), the proliferation rate would have to be substantially diminished in this early phase of the GC reaction. It is very unlikely that this is really the case, since the proliferation rate has been frequently measured to be of the order of $1/(6hr)$, and this value was found at different moments of the GC reaction (Hanna, 1964; Zhang *et al.*, 1988; Liu *et al.*, 1991).

Non-local centroblast-FDC interaction As has been shown, centroblast-specific differentiation scenarios, even being combined with an attractor which incorporates an inhomogeneity into the GC volume, do not lead to the expected appearance of dark zones. A centroblast differentiation process which is governed by a local interaction with FDCs leads to conceptual problems concerning the centroblast proliferation rate.

Therefore, in a fourth scenario, a nonlocal interaction of centroblasts and FDCs is investigated in order to find the experimentally observed morphology. Such a nonlocal interaction may be mediated by a diffusing signal molecule which is produced by the FDCs during the GC reaction. Each time when a centroblasts meets a threshold density of signal molecules it starts to differentiate into centrocytes at a certain rate. The signal molecules that initiated the differentiation process are not eliminated from the lattice, because they are not consumed by the centroblasts. The model then predicts a short appearance of a dark zone which is depleted within hours. The fast depletion is due to the large diffusion constant for the signal molecule in comparison to the diffusion constant of centroblasts.

Therefore, the signal molecules become homogeneously distributed on the whole GC volume, especially in the dark zone, within a short time. A homogeneous distribution of the differentiation signal is undistinguishable from the first scenario *Centroblast specific differentiation*: All centroblasts differentiate into centrocytes, independently of their position. Consequently, the dark zone is destroyed in the same way as in the scenario discussed before. In the present scenario dark zones cannot survive until the diffusion constant of the signal molecules is reduced to an unreasonable small value.

This leads us to a fifth scenario which builds upon the previous one by incorporating the consumption of signal molecules. It is rather plausible that the signal molecules have to bind to the centroblasts in order to initiate the differentiation process. Then, bound molecules are not available for a second initiation of centroblast differentiation as they have been before. We investigated this scenario in the model: As the FDC network is the source of signal molecules, only the centroblasts at the surface of the dark zone go into interaction with the differentiation signal and consume it. Therefore, the nucleus of the dark zone is widely protected against contact with signal molecules and can survive for significantly longer periods.

A representative simulation result is shown in Fig. 3: A large amount of proliferating centroblasts develops from 3 seeder cells. Those centroblasts which are placed beside the FDC network give rise to the dark zone (in the lower hemisphere). The dark zone is stable for a certain time and *evaporates* cells at its surface by differentiation into centrocytes in dependence on the diffusing signal molecules. The centrocytes generated at the interphase of the dark and the light zone tend to diffuse into the FDC network. The resulting life time of the dark zone directly depends on the production rate of signal molecules. When the dark zone has disappeared, centroblasts and centrocytes are distributed more or less homogeneously on the GC volume. During the remaining time the GC reaction declines.

Summarizing, we find two conditions which are together sufficient for the appearance of dark zones:

1. A monoclonal expansion of centroblasts beyond the FDC network.
2. A nonlocal interaction between FDCs and centroblasts, which may be realized with a differentiation signal molecule which is produced by FDCs and bound by centroblasts.

As has already been argued at the beginning of this section (see the subsection on *FDC inhomogeneity*) condition 1 is also a necessary condition for the development of the dark zone. However, concerning the non-locality of the centroblast-FDC interaction the situation is less clear and the argument for the necessity of this condition is a negative one: All alternative scenarios for the centroblast differentiation process lead to conceptual problems. As a consequence, non-locality cannot be deduced to be an imperative feature of the centroblast-FDC interaction. Nevertheless, the reader may agree that the presented scenario is an attractive and plausible way to explain the development of dark zones in GC reactions as it has been observed in experiment.

3.2 The reference germinal center

After having determined features of GC reactions that are sufficient for the development of dark zones, a reference GC can be defined. As we are dealing with a stochastic model we have to analyse ensembles of simulations with the same set of parameters but different generators of random numbers. Therefore, the results will always be given with an uncertainty corresponding to one standard deviation. The parameters in Tab. 1 that were mostly determined in Sec. 2, are used as a reference system. Nevertheless, some values had to be determined by an iterative optimization procedure depending on the outcome of the model. All simulations were done with time steps of 0.004 hr . A dependence of the results on the time resolution has not been observed in this regime. In each time step all lattice points are actualized in a random sequence. In the following, the general character of the reference GC will be shortly described. Special aspects will follow in the subsequent sections.

The simulation shows the three phases that were postulated: In the first phase the three seeder cells proliferate, so that the B-cell population grows exponentially. After 3 days the increase is slowed down due to spatial restrictions and due to the start of the centroblast differentiation process, which is governed by the signal molecules produced by the FDCs. The dark zone develops as shown in the previous section and vanishes at day 8.2 ± 0.4 (see Sec. 3.3). The selection of centrocytes takes place in the environment of the FDCs (see Fig. 4). At day 5 the production of output cells is started. It has been observed in experiment that between day 6 and 12 of the reaction the number of output cells multiplies 6-fold (Han *et al.*, 1995b). In the model this number is 5.9 ± 1.2 . The whole GC population, i.e. proliferating B-cells and centrocytes, decreases during this last phase and reaches a final number of 49 ± 29 proliferating B-cells after 21 days of the reaction. This number is influenced by the variation (within the physiological constraints) of the speed of the selection process, especially by changes of the centroblast differentiation rate (see also Sec. 3.5).

3.3 Duration of the dark zone

Experimentally, the dark zone has been observed in a lot of different GCs. It has been observed that the dark zone is already present 4 or 5 days after immunization and vanishes approximately at day 8 (Camacho *et al.*, 1998). In the latter experiment no dark zone has been observed at later times. Nevertheless, it remains unclear if this observation is independent of the system under consideration and of the experimental conditions. GCs with long lasting dark zones may exist. On the other hand, one may suspect that the complete absence of a dark zone is a sign for a malignant immune reaction (Loeffler & Stein, 2001).

In the following we will analyse what determines the duration of the intermediate appearance of dark zones. It is obvious that the amount of signal molecules in the GC will influence the speed of dark zone reduction by centroblast differentiation. In order to

quantify this statement, the dark zone is said to have vanished if the number of centrocytes in the lower hemisphere dominates the number of centroblasts. In Fig. 5 this corresponds to the crossing of the relative centroblast and centrocyte populations. The dark zone vanishes at day 8.2 ± 0.4 . A variation of the signal molecule production rate (or equivalently of the threshold concentration that is necessary to induce centroblast differentiation) shows that the life time of the dark zone indeed depends on this parameter (see Fig. 5 (b) and (c)). Principally, all durations of dark zones may be produced by a corresponding choice of the signal production rate. Therefore, the concept of non-local centroblast-FDC interaction allows intermediate dark zones as well as dark zones which remain stable during the whole GC reaction.

The duration of the dark zone is also influenced by other physiological magnitudes. One finds an interesting interplay of the signal production rate, the rate of centroblast differentiation, and the rate of centrocyte apoptosis. A slower centroblast differentiation prolongs the total GC reaction, i.e. more B-cells remain after 21 days. Naturally, this especially applies to the duration of the dark zone.

The apoptosis rate has a slightly more complex effect. This rate is the inverse centrocyte life time which, at the same time, determines how much time a centrocyte is given to be rescued from apoptosis by interaction with FDCs. A smaller apoptosis rate of $1/(10hr)$ would still be in accordance with experiment (Liu *et al.*, 1994). We observe that the prolonged life time of centrocytes has two basic effects: the duration of the dark zone is shortened and the total cell population is increased, so that the total GC reaction is prolonged. The latter effect is rather intuitive, as the death rate of centrocytes is reduced. At the same time this implies that, in average, the number of centrocytes is increased, especially, when compared to the number of centroblasts. Since the moment of breakdown of the dark zone is defined by the relative numbers of centroblasts and centrocytes, the duration of the dark zone is shortened in this way.

This section is concluded with the remark, that the presented non-local concept for centroblast differentiation is compatible with almost all intermediate or non-intermediate appearances of GC dark zones. The moment of dark zone destruction is basically determined by the (experimentally unknown) signal production rate, the centroblast differentiation rate, and the life time of centrocytes.

3.4 Optimal optimization

Until here, the origin of the dark zone has been enlightened and its stability during the GC reaction has been analysed. Now, the interest turns towards its function in the GC reaction, especially for the affinity maturation process. At first, the affinity maturation process will be described from the point of view of the model. Then the interplay of recycling and dark zone, and its importance for affinity maturation will be pointed out. Finally, the influence of the dark zone on the achieved affinity to the antigen will be discussed.

3.4.1 Affinity maturation

Among the major tasks of the GC reaction is the optimization of the antibody type with respect to the presented antigen and the production of plasma cells which secrete these optimized antibodies. Therefore, it is important to verify that a model which aims to help understand the origin and the function of the GC morphology also describes the affinity maturation process. B-cells are considered high affinity cells if they have at least a 30% probability to bind the antigen in the sense of Eq. (1), i.e. if $a(\phi, \phi^*) > 0.3$. The time course of the thus defined fraction of high affinity cells is depicted in Fig. 6. After about 9.4 ± 1.4 days the high affinity cells dominate in the GC, which compares to about 8 days observed in experiment (Jacob *et al.*, 1993).

Figs. 6 and 9 show that the kinetics of the fraction of high affinity B-cells can be grouped into four phases: During the phase of monoclonal expansion no high affinity B-cells exist at all. As no somatic hypermutation takes place at this time, no high affinity cells may emerge. When the mutation begins after 3 days, the number of high affinity B-cells grows in a controlled way. It then turns to a steep increase and finally reaches a plateau on a high level for the last days of the GC reaction. In the following the relation of this general behavior to some characteristic features of the GC reaction is discussed.

3.4.2 The role of recycling

The importance of recycling for affinity maturation has already been emphasized (Kepler & Perelson, 1993; Oprea *et al.*, 2000). Furthermore, it has been shown using a dynamical model without space resolution that a large recycling probability is necessary in order to get a reliable optimization process (Meyer-Hermann *et al.*, 2001). As has already been mentioned, the model considers those B-cells as recycled which have been positively selected, at least once, in interaction with FDCs and which restart to proliferate. This does not mean that these cells reenter the dark zone. On the contrary, the model predicts that recycling occurs in the light zone and – most interestingly – that recycled cells remain in the light zone and do not return to the dark zone, as was suspected several times (Kelsoe, 1996; Han *et al.*, 1997). This can clearly be seen in Fig. 4: the recycled cells all remain in the light zone.

The kinetics of the fraction of non-recycled and recycled B-cells is shown in Fig. 7. In the beginning the population of proliferating B-cells is dominated by non-recycled B-cells, and recycling does not play an important role. After 10.0 ± 0.5 days the proliferating cells are composed by equal parts of non-recycled and recycled B-cells. After 13.7 ± 1.2 days the non-recycled B-cell population vanishes. Afterwards, all proliferating B-cells are recycled cells, i.e. they are stemming from at least one positive selection.

The interpretation of this result is quite obvious. Until day 10 of the GC reaction an important part of the optimization procedure has already taken place (see Fig. 6). This is in accordance with the experimental observation that at this time the GC is already dominated by good cells (Jacob *et al.*, 1993). As a consequence, recycling does not seem

to be of great importance for the affinity maturation process at this time. If one stopped the GC reaction at this time, the cell population would have a higher average affinity to the antigen than the seeder cells. Nevertheless, the number of *optimal* cells would still be small and also a lot of low affinity cells would remain in the GC. The situation completely changes afterwards, when the dark zone has disappeared, and non-recycled B-cells become dominated by recycled B-cells. At this stage no low affinity cells are present in the GC anymore and there remains a slowly decreasing population of already positively selected B-cells.

Note that the average number of mutations of B-cells that differentiate into output cells is about 3 when the dark zone vanishes and about 9 at the end of the GC reaction – which is in accordance with experiment (Küppers *et al.*, 1993; Wedemayer *et al.*, 1997). It follows that about 2/3 of all mutations in B-cells, that do not die by apoptosis but are selected and differentiate into output cells later on, occur in recycled B-cells. As can be seen in Fig. 8, these late mutations are not useless fluctuations of the affinity but still substantially increase the affinity to the antigen. This reveals that a major part of the affinity maturation process is realized during domination of the recycled B-cells. Consequently, recycling is not only the basis for the multiplication of those cells which are already of relatively high quality but also for the fine tuning of these cells which appears to be a relevant part of the affinity maturation process.

3.4.3 The role of the dark zone

One can observe an interesting correlation between the moment when recycled B-cells dominate over non-recycled centroblasts in the GC and the onset of the steep growth phase (mentioned at the beginning of this section) of the average cell affinity to the antigen (compare Fig. 6 and 7, 9 (a) and (c), as well as 9 (b) and (d)). The domination of recycled B-cells has to be preceded by the destruction of the dark zone which is indeed the case. Therefore, the phase of accelerated growth of average affinity in the GC is not primarily due to an accelerated affinity maturation but to the elimination of low affinity cells which still proliferate in the dark zone. Note that when the non-recycled centroblasts are completely eliminated from the GC, the average cell affinity already reaches a plateau.

As a second interesting observation, the affinity development of all produced output cells and of centroblasts and centrocytes differs considerably. Before the steep increase in average affinity the output cells are of better quality than the proliferating B-cells – afterwards the proliferating B-cells are better or at least equally good (see Fig. 9 (c), and (d)). Note that the affinity of centroblasts and centrocytes has to become larger than the affinity of the already produced output cells. Otherwise, a further increasing quality of all produced output cells together becomes impossible.

Taking both observations together one is led to the following hypothesis: The affinity gap between the cells in the dark and the light zone becomes larger during the GC reaction, and in the late phase of the GC reaction a further enhancement of the total affinity is inhibited by the low affinity cells in the dark zone. Consequently, the dark zone has to be

dissolved in time in order to optimize the affinity maturation process.

If this hypothesis holds true, a correlation should exist between the fraction of high affinity output cells (averaged over the whole GC reaction) and the duration of the dark zone. This can be studied by varying the production rate s for the centroblast differentiation signal molecule, which is one of the parameters that control the life span of the dark zone. The parameters in Tab. 1 are used and the signal production rate is varied in the range of $6/hr \leq s \leq \infty$, where ∞ implies that the centroblasts receive the signal without any time delay. Since the final number of B-cells is influenced from these changes, the centroblast differentiation rate is adapted correspondingly: $5.5/hr \leq g_1 \leq 6.4/hr$. This ensures to find (in average) the same number of cells at the end of the GC reaction.

It is important to take care of comparability of the simulations, as in a stochastic model the quantitative results are variable to some extent. This is especially true for the final state of the GC reaction, i.e. the number of proliferating B-cells which remain in the GC at the end of the reaction. As can be seen in Fig. 10, the quality of the produced output cells (averaged over the whole GC reaction) clearly correlates with the final number of proliferating cells at day 21 of the reaction up to a certain level of those cells. Above that level the output cell quality seems to saturate. Therefore, an analysis concerning the correlation between the length of the dark zone and the output-quality has to be based on simulations with comparable final states, in order not to hide one correlation with another one. Consequently, only those simulations were taken into account that resulted in a reasonable number of remaining proliferating B-cells in the range of $50 \pm 1\sigma$, where the standard deviation σ is taken over all simulations. The resulting dependency of the total output quality (i.e. averaged over the whole GC reaction) on the duration of the dark zone is depicted in Fig. 11. Indeed, the fraction of high affinity output cells decreases if the dark zone remains stable for a too long period of more than 10 days. In conclusion, intermediate dark zones which vanish before day 10 of the GC reaction are advantageous for the affinity maturation process in GC reactions.

On the other hand, Fig. 11 shows that for too short living dark zones that vanish before day 7 of the reaction, the quality of all produced output cells is again reduced. This leads to the clear conclusion that the intermediate appearance of dark zones optimizes the affinity maturation process in GC reactions. The best results are found for dark zones that vanish between day 7 and 10 of the GC reaction.

Finally, the number of output cells resulting from the GC reaction is correlated with the dark zone duration. The maximum number of output cells is found for dark zones of exactly the same duration as that one required from the point of view of cell quality (see Fig. 11). Note, that the error bars are larger here than in the result for the output quality.

3.5 Evolution of the total volume

The evolution of the total GC volume during the GC reaction after primary immunization has been observed in experiment by measuring the follicle center volume in per cent of the

total splenic volume (Liu *et al.*, 1991) or the total GC volume itself (Hollowood & Macartney, 1992). In both cases a statistical average over a lot of GCs found in the spleen was performed. These measurements are suitable for comparison with the present model, even if the absolute numbers cannot be interpreted. The observed time course has the following properties: At first, the splenic GC volume increases steeply. It reaches a maximum at day 4 (Liu *et al.*, 1991) or day 5 (Hollowood & Macartney, 1992) of the reaction, and, subsequently, decreases until the end of the reaction at day 21. This qualitative behavior is perfectly reproduced by the model for intermediate dark zones that vanish between day 6.5 and 9.1 of the GC reaction (see Fig. 12). As in experiment, the model shows an exponential increase of the GC volume, that is slowing down around day 3 of the reaction and reaches its maximum at day 4. Finally, a fast decrease of the volume follows becoming more moderate in the late phase of the reaction. An interesting observation is that the time course of GC reactions with longer dark zones until day 14.1 quantitatively is not in accordance with the data found in experiment (see Fig. 12). This is another indication for an intermediate and relative short appearance of dark zones in GC reactions.

However, one important question remains unresolved in this context: How does the GC reaction end? In the framework of this model no mechanism was assumed in order to stop the reaction. The resulting final state of the reaction is a strongly decreased but, nevertheless, relatively stable population of B-cells. Therefore, we are led to the question if, eventually, there exists an additional mechanism that terminates the GC reaction.

Comparing the GC-volume with the already mentioned experiment (Liu *et al.*, 1991) we can find a first hint. It seems that in the last phase of the GC reaction the volume remains on a higher level than in the model and decreases faster at the very end (see Fig. 12). This behavior may be achieved in the model e.g. with a slower selection procedure which stabilizes the total B-cell population on a higher level. However, the model does not provide any possibility for the rapid population decrease during the last days, so that the reaction would remain on a high level after 21 days. This would have to be introduced separately, e.g. by incorporating a change of the proliferation rate or the recycling probability during the GC reaction. The latter one may be favored: It is believed that the differentiation process of positively selected centrocytes is determined by a local interaction with FDCs. It would not be very surprising if the proportion of the signals that induce recycling and differentiation into output cells changed during the GC reaction, for example in dependence on the already achieved level of affinity to the antigen.

In this context it is interesting to note that the total number of produced output cells (summed over the whole GC reaction) becomes larger if more proliferating B-cells remain in the GC during its last phase (see Fig. 10). This correlation indicates that a prolonged high number of B-cells that decreases rapidly at the very end of the reaction may be advantageous for the quantity of the GC output.

3.6 Robustness of the results

3.6.1 Stochastic variation

One should be aware of the fact that all simulations were based on the same FDC and seeder cell configuration. This has been necessary in order to uncover the GC features and dependencies on the model parameters. If the simulation is started by a stochastic process from the very beginning of the GC reaction the variability of the results becomes substantially larger. Especially, the specific correlations during the dynamic development of the GC reaction would partly be hidden by the variability of the state after 3 days of pure monoclonal expansion of centroblasts. This state is very sensitive to the initial cell distribution and to changes of the generator of random numbers, as the number of cells is very low during the first hours of the reaction. Therefore, slight differences at the beginning are crucial for the development and blow up when the GC further expands.

This restriction of stochasticity was useful, as the main interest was an analysis of the main part of the GC reaction. However, the variability of real healthy GCs may be substantially larger than shown here.

3.6.2 Affinity of seeder cells

As mentioned in Sec. 2.2 the seeder B-cells that initiate the GC reaction have a low but non-vanishing affinity to the antigen. In the presented simulation runs they have to mutate at least 5 times in order to find the optimal mutant. In this case one gets a rather stable answer measured in terms of the quality of the resulting cells. However, the number of necessary mutations starting from the initial state is crucial for the GC development. If the affinity of the seeder cells is too low, the optimal mutant remains unreached in the framework of the model. Consequently, the initial distribution of the seeder cells in the shape space is important for the outcome of the GC reaction (see also Meyer-Hermann et al., 2001).

It has been observed in experiments that GCs developing during an immune response can be divided into two classes: Either high affinity cells remain practically absent or they already dominate in an early stage of the reaction (Berek et al., 1991; Radmacher et al., 1998). This behavior may correspond to the above mentioned limits of high and low affinity seeder cells. It is the aim of current statistical investigation to decide if the model reproduces a sharp switch between the two observed GC classes or not.

3.6.3 Selection process

The affinity maturation process is basically governed by the centrocyte life time, the time a centrocyte needs to bind to an FDC, and the *total* selection time. The model results are indeed insensitive to a complementary change of the duration of different selection substate, i.e. one may increase the centrocyte differentiation rate and reduce the rate of centrocyte-FDC-dissociation, correspondingly. But the results are sensitive to a change of only one of these parameters or of the apoptosis rate. We conclude that in the framework of the model the duration of the different selection substates (starting from the binding

of centrocytes and FDCs and ending with the differentiated centrocyte) is not of direct relevance for the affinity maturation process. However, the total selection time turned out to be important.

3.6.4 Diffusion constants

The diffusion constants – besides the availability of space – determine the mobility of the B-cells in the GC volume. Unfortunately, their values for centroblasts and centrocytes are rather uncertain. Therefore, it is important to check the relevance of these parameters for the characterization of the GC reaction. If the mobility of the B-cells is larger, the total number of B-cells is increased in the late phase of the GC reaction. The B-cells get a higher chance of reaching an FDC and, in this way, have a higher chance of being selected. This becomes especially relevant in the late phase of the GC reaction as the density of cells becomes small and their mobility plays a major role. It is not surprising that for smaller diffusion constants the total number of cells is reduced in the late phase. Since the total number of produced output cells is directly related to the final number of B-cells (see Fig. 10) the produced output should not be interpreted in terms of absolute numbers.

The affinity maturation process is slightly influenced by the diffusion constants. A faster diffusion basically has the same effect as a slower apoptosis rate. However, the relation of the affinity maturation process to the dark zone is not altered.

The outcome of the simulations does not depend on the diffusion constant of the signal molecule until the values remain substantially larger than the diffusion constant of the B-cells.

4 Discussion

The aim of this article was to reveal the origin and the function of the specific morphology of the GC reaction. Concerning the origin, two requirements were found: It is essential for the development of dark zones that during the first phase of monoclonal expansion the centroblasts also occupy a volume besides the FDC network. Secondly, it was shown that a dark zone develops if the centroblast differentiation to centrocytes is governed by a signal molecule, which is produced by the FDCs and consumed by the centroblasts. This is surely not the only possible scenario. However, the non-local character of the interaction between cells outside the dark zone and centroblasts is an essential ingredient. It has been shown that other obvious concepts for the centroblast differentiation lead to contradictions with experimental observations. For example, centroblast-specific differentiation does not allow for the development of dark zones at all, even with a centrocyte attractor in the FDC network. A local centroblast-FDC interaction leads to a dominance of centroblasts that is completely untypical in real GC reaction. This concept may be restored if one introduces an early decreasing proliferation rate, which again is not in agreement with experimental data.

The concept of non-local centroblast-FDC interaction is compatible with dark zones of different durations, i.e. with stable or intermediate dark zones. Intermediately appearing dark zones have been observed in experiment (Camacho *et al.*, 1998). In order to understand the function of the dark zone, the quality of the B-cells resulting from the GC reaction with respect to the antigen, i.e. the quality of the affinity maturation process, has been examined. We showed that the affinity maturation process is inhibited if the dark zone does not vanish until day 10 of the GC reaction. Shorter dark zones lead to a better optimization process and, consequently, to plasma- and memory-cells of higher quality. On the other hand, the dark zone has to exist until day 7 of the GC reaction in order to optimize the affinity maturation process. Also, the quantity of produced plasma- and memory-cells were found to be maximized for dark zones of exactly this duration. These results suggest that the dark zone has the function to present a large pool of different B-cells with a great diversity to the FDCs for selection, and at the same time to increase the total number of resulting antibody-producing cells. Therefore, the development of a dark zone as well as its depletion in time are essential elements of the affinity maturation process.

The time course of the GC volume predicted by the model was compared to experimentally observed GC volumes. The model results are in agreement with experiment for dark zones that vanish between day 6.5 and 9.1 of the GC reaction. This supports the above argument for the existence of an intermediate dark zone, and suggests that nature has chosen to realize GCs with exactly this property. So the main conclusion of this analysis is that affinity maturation is optimized for intermediate dark zones that vanish around day 8 of the GC reaction, and that it seems that this optimal procedure has been realized in existing GCs.

In accordance with previous works, recycling, i.e. the process that centrocytes re-proliferate, turned out to be essential for a well working affinity maturation. More explicitly, the affinity maturation process is divided into a phase of rough optimization which is dominated by B-cells in the dark zone and into a phase of fine tuning which is dominated by recycled B-cells. It is worth emphasizing in this context, that the number of recycled B-cells that reenter the dark zone is negligible.

At this point one should think about the optimization of the model. The present model is in accordance with experimentally observed GCs, especially including quantitative statements. Also the time course of the GC volume has been found to be in agreement with experiment and supports the hypothesis of an intermediate dark zone of relatively short duration. The total GC volume is reduced to a reasonable small number of remaining cells without any changes in the dynamical parameters. However, the quality of the resulting plasma- and memory-cells is enhanced and their quality is increased if the total number of B-cells remains larger than in the model during the last days of the GC reaction. This points towards an additional mechanism that stops the GC reaction at the very end of the reaction. It was argued, that a recycling probability which is reduced depending on the already achieved affinity maturation is a good candidate. Also the production of

antibodies inside the GC and the implied binding of antigen fragments may be considered in this context.

Finally, the role of T-helper cells should be investigated. They are believed to have an important influence on the selection process as well as on the inhibition of apoptosis (Lindhout *et al.*, 1995; Brandtzaeg, 1996; Tew *et al.*, 1997; Hollmann & Gerdes, 1999; Hur *et al.*, 2000; van Eijk *et al.*, 2001). Therefore, T-helper cells should be considered if one is interested in the details of the selection process, which did not turn out to be of primary importance for the development of the dark zone analysed in the present article. In addition, T-helper cells instead of the FDCs are also a good candidate to produce the centroblast differentiation signal (Dubois *et al.*, 1999a, 1999b), that has been postulated here.

References

- BEREK, C. & MILSTEIN, C., 1987: Mutation drift and repertoire shift in the maturation of the immune response, *Immunol. Rev.* **96**, 23-41.
- BEREK, C., BERGER, A. & APEL, M., 1991: Maturation of the Immune Response In Germinal Centers, *Cell* **67**, 1121-1129.
- BEREK, C., 2001: private communication.
- BEYER, T. & MEYER-HERMANN, M., 2002: A corresponding work is currently in preparation.
- BRANDTZAEG, P., 1996: The B-cell development in tonsillar lymphoid follicles, *Acta Otolaryngol. Suppl. (Stockh)* **523**, 55-59.
- CAMACHO, S.A., KOSCOVILBOIS, M.H. & BEREK, C., 1998: The Dynamic Structure of the Germinal Center, *Immunol. Today* **19**, 511-514.
- CHOE, J. & CHOI, Y.S., 1998: IL-10 Interrupts Memory B-Cell Expansion in the Germinal Center by Inducing Differentiation into Plasma-Cells, *Eur. J. Immunol.* **28**, 508-515.
- CHOE, J., LI, L., ZHANG, X., GREGORY, C.D. & CHOI, Y.S., 2000: Distinct Role of Follicular Dendritic Cells and T Cells in the Proliferation, Differentiation, and Apoptosis of a Centroblast Cell Line, L3055, *J. Immunol.* **164**, 56-63.
- DUBOIS, B., BARTHÉLÉMY, C., DURAND, I., LIU, Y.-J., CAUX, C. & BRIÈRE, F., 1999a: Toward a Role of Dendritic Cells in the Germinal Center Reaction – Triggering of B-Cell Proliferation and Isotype Switching, *J. Immunol.* **162**, 3428-3436.
- DUBOIS, B., BRIDON, J.-M., FAYETTE, J., BARTHÉLÉMY, C., BANCHEREAU, J., CAUX, C. & BRIÈRE, FRANCINE, 1999b: Dendritic Cells directly modulate B cell growth and differentiation, *J. Leukoc. Biol.* **66**, 224-230.
- DUNN-WALTERS, D., THIEDE, C., ALPEN, B. & SPENCER, J., 2001: Somatic hypermutation and B-cell lymphoma, *Philos. Trans. R. Soc. Lond. B Biol. Sci.* **356**, 73-82.
- FALINI, B. ET AL., 2000: A monoclonal antibody (MUM1p) detects expression of the MUM1/IRF4 protein in a subset of germinal center B cells, plasma cells, and activated T cells, *Blood* **95**, 2084-2092.
- HAN, S.H., ZHENG, B., DAL PORTO, J. & KELSOE, G., 1995a: In situ Studies of the Primary Immune Response to (4-Hydroxy-3-Nitrophenyl) Acetyl IV. Affinity-Dependent, Antigen-Driven B-Cell Apoptosis in Germinal Centers as a Mechanism for Maintaining Self-Tolerance, *J. Exp. Med.* **182**, 1635-1644.
- HAN, S.H., HATHCOCK, K., ZHENG, B., KELPER, T.B., HODES, R. & KELSOE, G., 1995b: Cellular Interaction in Germinal Centers: Roles of CD40-Ligand and B7-1 and B7-2 in Established Germinal Centers, *J. Immunol.* **155**, 556-567.
- HAN, S., ZHENG, B., TAKAHASHI, Y. & KELSOE, G., 1997: Distinctive characteristics of germinal center B cells, *Immunology* **9**, 255-260.
- HANNA, M.G., 1964: An autoradiographic study of the germinal center in spleen white

- pulp during early intervals of the immune response, *Lab. Invest.* **13**, 95-104.
- HOLLMANN, C. & GERDES, J., 1999: Follicular Dendritic Cells and T-Cells – Nurses and Executioners in the Germinal Center Reaction, *J. Pathol.* **189**, 147-149.
- HOLLOWOOD, K. & MACARTNEY, J., 1992: Cell kinetics of the germinal center reaction – a stathmokinetic study, *J. Immunol.* **22**, 261-266.
- HOSTAGER, B.S., CATLETT, I.M. & BISHOP, G.A., 2000: Recruitment of CD40 and Tumor Necrosis Factor Receptor-associated Factors 2 and 3 to Membrane Microdomains during CD40 Signaling, *J. Biol. Chem.* **275**, 15392-15398.
- HUR, D.H., KIM, D.J., KIM, S., KIM, Y.I., CHO, D., LEE, D.S., HWANG, Y.-I., BAE, K.-W., CHANG, K.Y. & LEE, W.J., 2000: Role of follicular dendritic cells in the apoptosis of germinal center B cells, *Immunol. Lett.* **72**, 107-111.
- JACOB, J., KASSIR, R. & KELSOE, G., 1991: In situ studies of the primary immune response to (4-hydroxy-3-nitrophenyl)acetyl. I. The architecture and dynamics of responding cell populations, *J. Exp. Med.* **173**, 1165-1175.
- JACOB, J., PRZYLEPA, J., MILLER, C. & KELSOE, G., 1993: In situ studies of the primary response to (4-hydroxy-3-nitrophenyl)acetyl. III. The kinetics of V region mutation and selection in germinal center B cells, *J. Exp. Med.* **178**, 1293-1307.
- KELSOE, G., 1996: The germinal center: a crucible for lymphocyte selection, *Semin. Immunol.* **8**, 179-184.
- KEPLER, T.B. & PERELSON, A.S., 1993: Cyclic re-entry of germinal center B cells and the efficiency of affinity maturation, *Immunol. Today* **14**, 412-415.
- KESMIR, C. & DE BOER, R.J., 1999: A Mathematical Model on Germinal Center Kinetics and Termination, *J. Immunol.* **163**, 2463-2469.
- KOOPMAN, G., KEEHNEN, R.M., LINDHOUT, E., ZHOU, D.F., DE GROOT, C. & PALS, S.T., 1997: *Eur. J. Immunol.* **27**, 1-7.
- KROESE, F.G., WUBBENA, A.S., SEIJEN, H.G. & NIEUWENHUIS, P., 1987: Germinal centers develop oligoclonally, *Eur. J. Immunol.* **17**, 1069-1072.
- KÜPPERS, R., ZHAO, M., HANSMANN, M.L. & RAJEWSKY, K., 1993: Tracing B Cell Development in Human Germinal Centers by Molecular Analysis of Single Cells Picked from Histological Sections, *EMBO J.* **12**, 4955-4967.
- LINDHOUT, E., LAKEMAN, A. & DE GROOT, C., 1995: Follicular dendritic cells inhibit apoptosis in human B lymphocytes by rapid and irreversible blockade of preexisting endonuclease, *J. Exp. Med.* **181**, 1985-1995.
- LINDHOUT, E., KOOPMAN, G., PALS, S.T. & DE GROOT, C., 1997: Triple check for antigen specificity of B cells during germinal centre reactions, *Immunol. Today* **18**, 573-576.
- LIU, Y.J., BARTHELEMY, C., DE BOUTELLER, O. & BANCHEREAU, J., 1994: The differences in survival and phenotype between centroblasts and centrocytes, *Adv. Exp. Med. Biol.* **355**, 213-218.
- LIU, Y.J., JOSHUA, D.E., WILLIAMS, G.T., SMITH, C.A., GORDON, J. & MACLENNAN, I.C., 1989: Mechanism of antigen-driven selection in germinal centres, *Nature*

342, 929-931.

- LIU, Y.J., ZHANG, J., LANE, P.J., CHAN, E.Y. & MACLENNAN, I.C.M., 1991: Sites of specific B cell activation in primary and secondary responses to T cell-dependent and T cell-independent antigens, *Eur. J. Immunol.* **21**, 2951-2962.
- LOEFFLER, M. & STEIN, H., 2001: private communication.
- MACLENNAN, I.C.M., 1994: Germinal Centers, *Annu. Rev. Immunol.* **12**, 117-139.
- MCHEYZER-WILLIAMS, M.G., MCLEAN, M.J., LABOR, P.A. & NOSSAL, G.V.J., 1993: Antigen-driven B cell differentiation in vivo, *J. Exp. Med.* **178**, 295-307.
- MEYER-HERMANN, M., DEUTSCH, A. & OR-GUIL, M., 2001: Recycling Probability and Dynamical Properties of Germinal Center Reactions, *J. Theor. Biol.* **210**, 265-285.
- MEYER-HERMANN, M., 2002: Does Recycling in Germinal Centers exist?, *Immunol. Cell Biol.* **80**, 30-35.
- MURRAY, J.D., 1993: *Mathematical Biology*. Springer, Berlin u.a., 2. Aufl.
- NOSSAL, G., 1991: The molecular and cellular basis of affinity maturation in the antibody response, *Cell* **68**, 1-2.
- OPREA, M. & PERELSON, A.S., 1996: Exploring the Mechanism of Primary Antibody Responses to T-Cell-Dependent Antigen, *J. Theor. Biol.* **181**, 215-236.
- OPREA, M. & PERELSON, A.S., 1997: Somatic mutation leads to efficient affinity maturation when centrocytes recycle back to centroblasts, *J. Immunol.* **158**, 5155-5162.
- OPREA, M., VAN NIMWEGEN, E. & PERELSON, A.S., 2000: Dynamics of One-pass Germinal Center Models: Implications for Affinity Maturation, *Bull. Math. Biol.* **62**, 121-153.
- PASCUAL, V., LIU, Y.-J., MAGALSKI, A., DE BOUTEILLER, O., BANCHEREAU, J. & CAPRA, J.D., 1994a: Analysis of somatic mutation in five B cell subsets of human tonsil, *J. Exp. Med.* **180**, 329-339.
- PASCUAL, V., CHA, S., GERSHWIN, M.E., CAPRA, J.D. & LEUNG, P.S.C., 1994b: Nucleotide Sequence Analysis of Natural and Combinatorial Anti-PDC-E2 Antibodies in Patients with Primary Biliary Cirrhosis, *J. Immunol.* **152**, 2577-2585.
- PERELSON, A.S. & OSTER, G.F., 1979: Theoretical Studies of Clonal Selection: Minimal Antibody Repertoire Size and Reliability of Self-Non-self Discrimination, *J. Theor. Biol.* **81**, 645-670.
- RADMACHER, M.D., KELSOE, G. & KEPLER, T.B., 1998: Predicted and Inferred Waiting-Times for Key Mutations in the Germinal Center Reaction – Evidence for Stochasticity in Selection, *Immunol. Cell Biol.* **76**, 373-381.
- RUNDELL, A., DECARLO, R., HOGENESCH, H. & DOERSCHUK, P., 1998: The Humoral Immune-Response to Haemophilus-Influenzae Type-B – A Mathematical-Model Based on T-Zone and Germinal Center B-Cell Dynamics, *J. Theor. Biol.* **194**, 341-381.
- SIEPMANN, K., SKOK, J., VAN ESSEN, D., HARNETT, M. & GRAY, D., 2001: Rewiring of CD40 is necessary for delivery of rescue signals to B cells in germinal centres and subsequent entry into the memory pool, *Immunol.* **102**, 263-272.
- SKALAK, R. & CHIEN, S., 1987: *Handbook of Bioengineering*. McGraw-Hill, New York

et al.

- TEW, J. & MANDEL, T., 1979: Prolonged antigen half-life in the lymphoid follicles of specifically immunized mice, *Immunology* **37**, 69-76.
- TEW, J.G., WU, J., QIN, D., HELM, S., BURTON, G.F. & SZAKAL, A.K., 1997: Follicular dendritic cells and presentation of antigen and costimulatory signals to B cells, *Immunol. Rev.* **156**, 39-52.
- VAN EIJK, M. & DE GROOT, C., 1999: Germinal Center B-Cell Apoptosis Requires Both Caspase and Cathepsin Activity, *J. Immunol.* **163**, 2478-2482.
- VAN EIJK, M., MEDEMA, J.P. & DE GROOT, C., 2001: Cellular Fas-Associated Death Domain-Like IL-1-Converting Enzyme-Inhibitory Protein Protects Germinal Center B Cells from Apoptosis During Germinal Center Reactions, *J. Immunol.* **166**, 6473-6476.
- WEDEMAYER, G.J., PATTEN, P.A., WANG, L.H., SCHULTZ, P.G. & STEVENS, R.C., 1997: Structural insights into the evolution of an antibody combining site, *Science* **276**, 1665-1669.
- ZHANG, J., MACLENNAN, I.C.M., LIU, Y.J. & LAND, P.J.L., 1988: Is rapid proliferation in B centroblasts linked to somatic mutation in memory B cell clones, *Immunol. Lett.* **18**, 297-299.

Acknowledgments

I thank Tilo Beyer and Andreas Deutsch for intense discussions and valuable comments.

Parameter	symbol	physiological	assumed
Shape space dimension	d_s		4
Width of Gaussian affinity weight function	Γ	<i>2.8</i>	
Lattice constant	Δx		$10 \mu m$
Radius of GC	R	$220 \mu m$	
Number of seeder cells		3	
Diffusion constant for centroblasts	D_{CB}	$5 \frac{\mu m^2}{hr}$	
Ratio of centroblast to centrocyte radius	$\frac{r_{CB}}{r_{CC}}$	3	
Diffusion constant of signal molecules	D_{sig}	$200 \frac{\mu m^2}{hr}$	
Number of FDCs		20	
Length of FDC arms		$30 \mu m$	
Duration of phase of monoclonal expansion	Δt_1	72 hr	
Duration of optimization phase	Δt_2	48 hr	
Rate of proliferation (2D)	p	1/(9hr)	
Maximal distance for CB proliferation	R_P		$60 \mu m$
Mutation probability	m	0.5	
Rate of differentiation signal production by FDCs	s		$9/hr$
Rate of centroblast differentiation	g_1	1/(6hr)	
Rate of FDC-centrocyte dissociation	g_2	$1/2hr$	
Rate of differentiation of selected centrocytes	g_3	$1/(7hr)$	
Probability of recycling of selected centrocytes	q	<i>0.8</i>	
Rate of centrocyte apoptosis	z	$1/(7hr)$	

Table 1: Summary of all physiological and assumed magnitudes entering the 2D model. The parameters are classified in two basic categories: Those with a direct *physiological* interpretation and those which were *assumed* for conceptual reasons of the model. The physiological parameters are shown in bold, if they are known experimentally with a sufficient precision. If the parameter has a physiological counterpart and is not known experimentally but has been determined indirectly by the analysis of experimental data, the value is shown in italic. Note, that all given rates are the physiological ones which enter with an additional factor of $\ln(2)$ into the model. The symbols correspond to those used in the text.

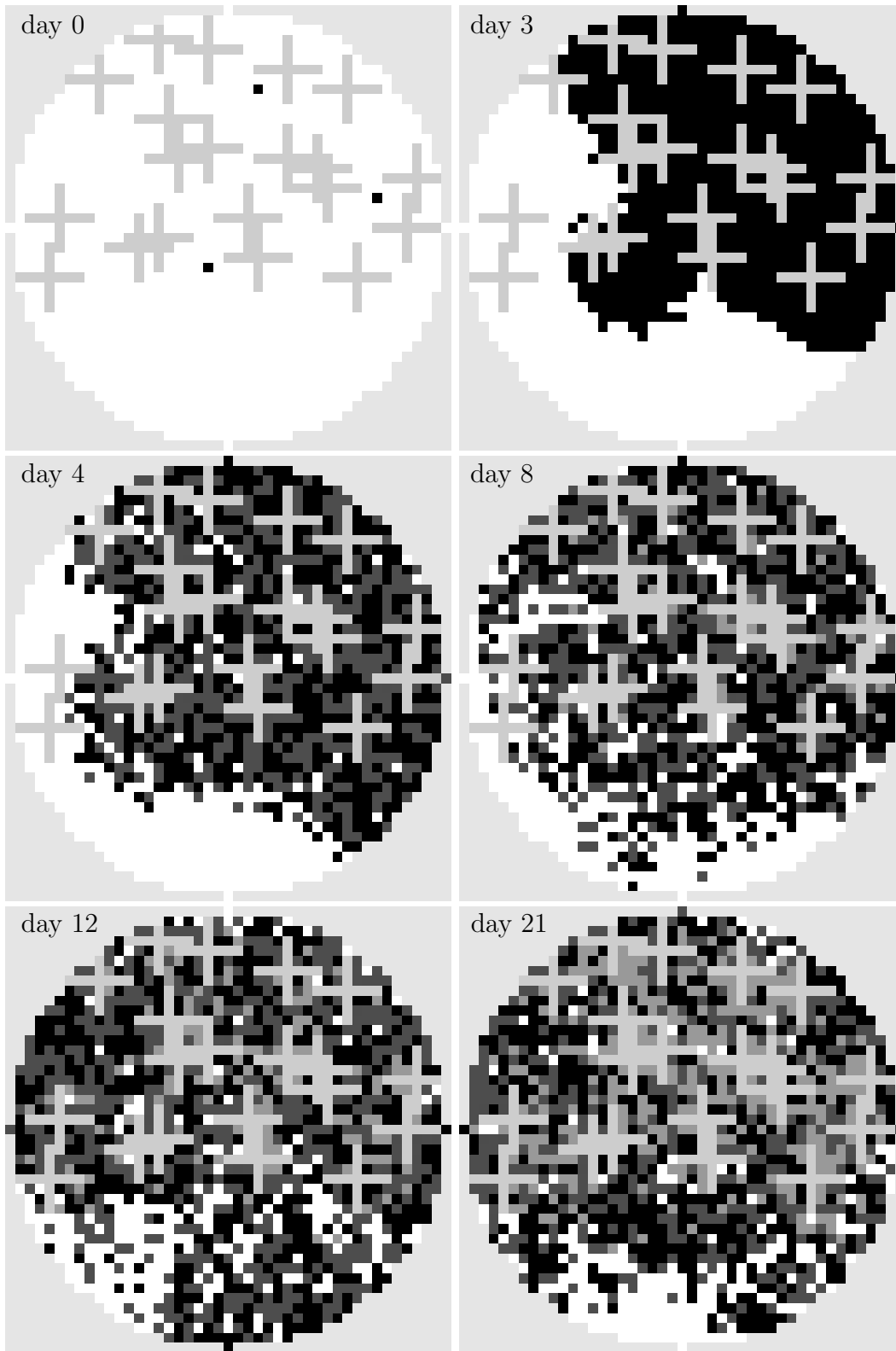


Figure 1: If the centroblast differentiation is independent of the FDCs (especially without differentiation signals) no dark zone appears during the GC reaction. This remains true even with a centrocyte attractor in the FDC network. Here, the centrocyte-FDC interaction time is $g_2^{-1} = 10 \text{ hr}$, and the centroblast differentiation rate is $g_1 = 1/(8.7 \text{ hr})$. All other parameters are like in Tab. 1. The initial distribution and the stages of the reaction after 3, 4, 8, 12, 21 days are shown. The represented cell types are (from dark to light): proliferating cells, centrocytes (in all stages of the selection process), output cells, FDCs, and empty space.

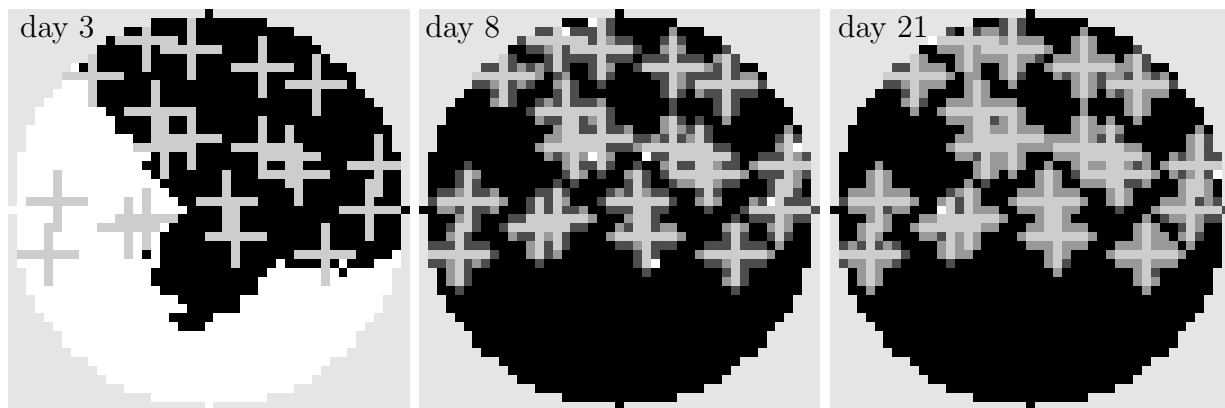


Figure 2: Using the concept of centroblast differentiation by local interaction with FDCs, the dark zone is established very early and is stable until the end of the GC reaction. The parameters are like in Tab. 1, except that the centroblast differentiation occurs in the moment of contact with FDCs (realistic differentiation rates further enhance the fraction of centroblasts) and that no differentiation signal exists. The stages of the reaction after 3, 8, 21 days are shown. The represented cell types are (from dark to light): proliferating cells, centrocytes (in all stages of the selection process), output cells, FDCs, and empty space.

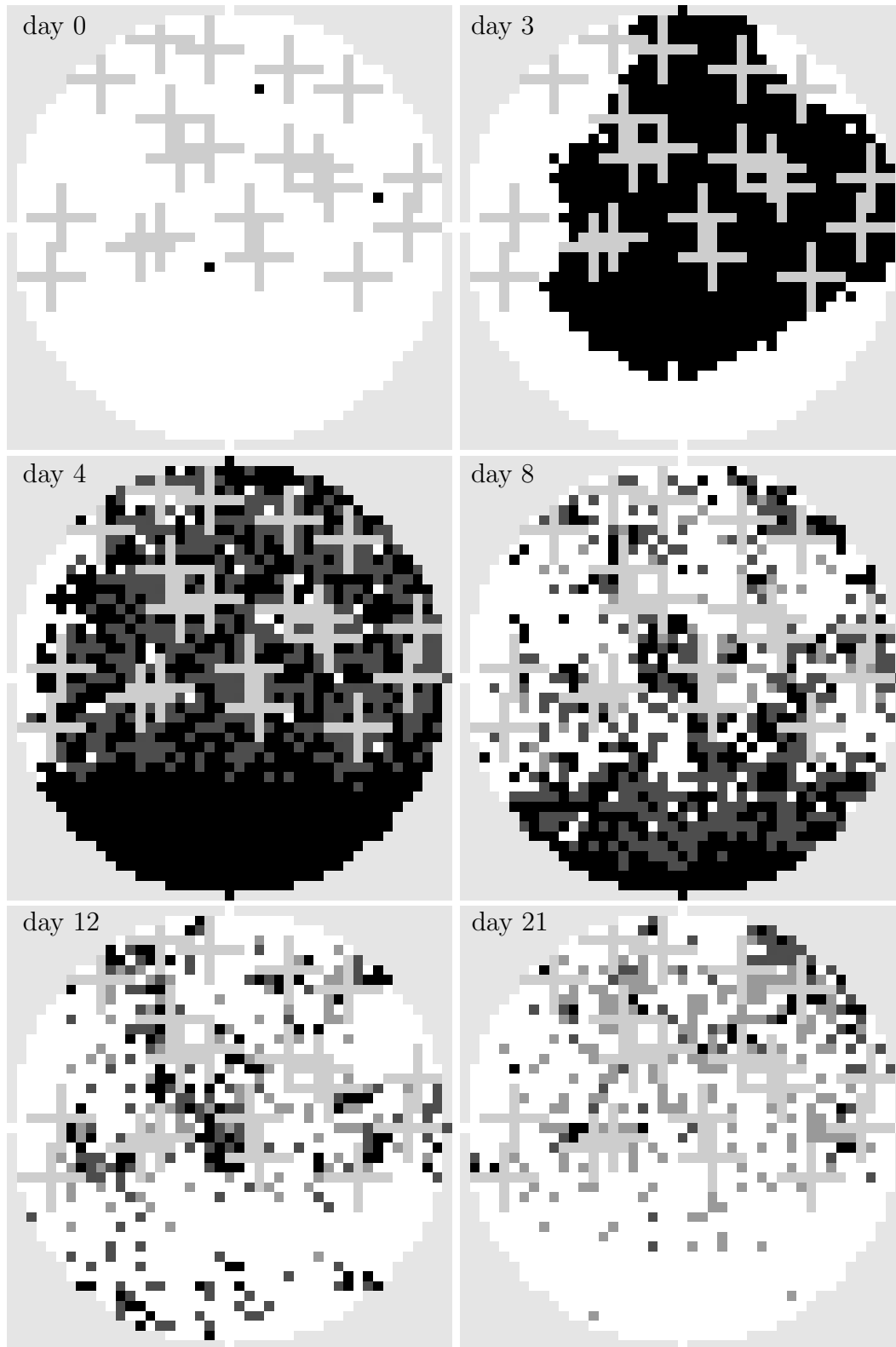


Figure 3: Development of the dark zone during a GC reaction: The initial distribution and the stages of the reaction after 3, 4, 8, 12, 21 days. The represented cell types are (from dark to light): proliferating cells, centrocytes (in all stages of the selection process), output cells, FDCs, and empty space. The used parameters are given in Tab. 1.

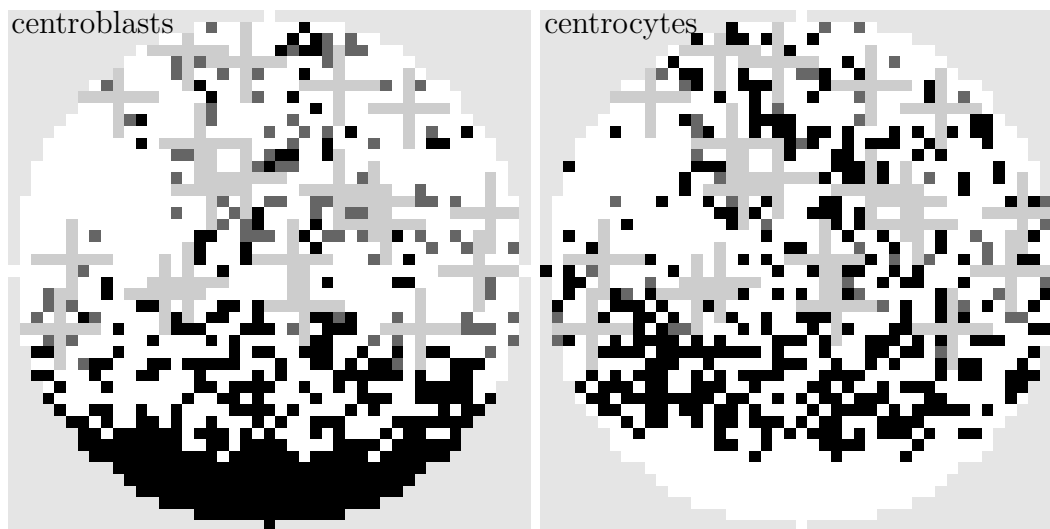


Figure 4: The same GC reaction as in Fig. 3 is shown at day 6 for proliferating cells (left) and centrocytes (right) separately. The recycled proliferating B-cells (grey, left figure) do not reenter the dark zone, where only non-recycled centroblasts (black, left figure) are found. The unselected centrocytes (black, right figure) are selected (grey, right figure) in the narrow neighborhood of the FDCs (light grey).

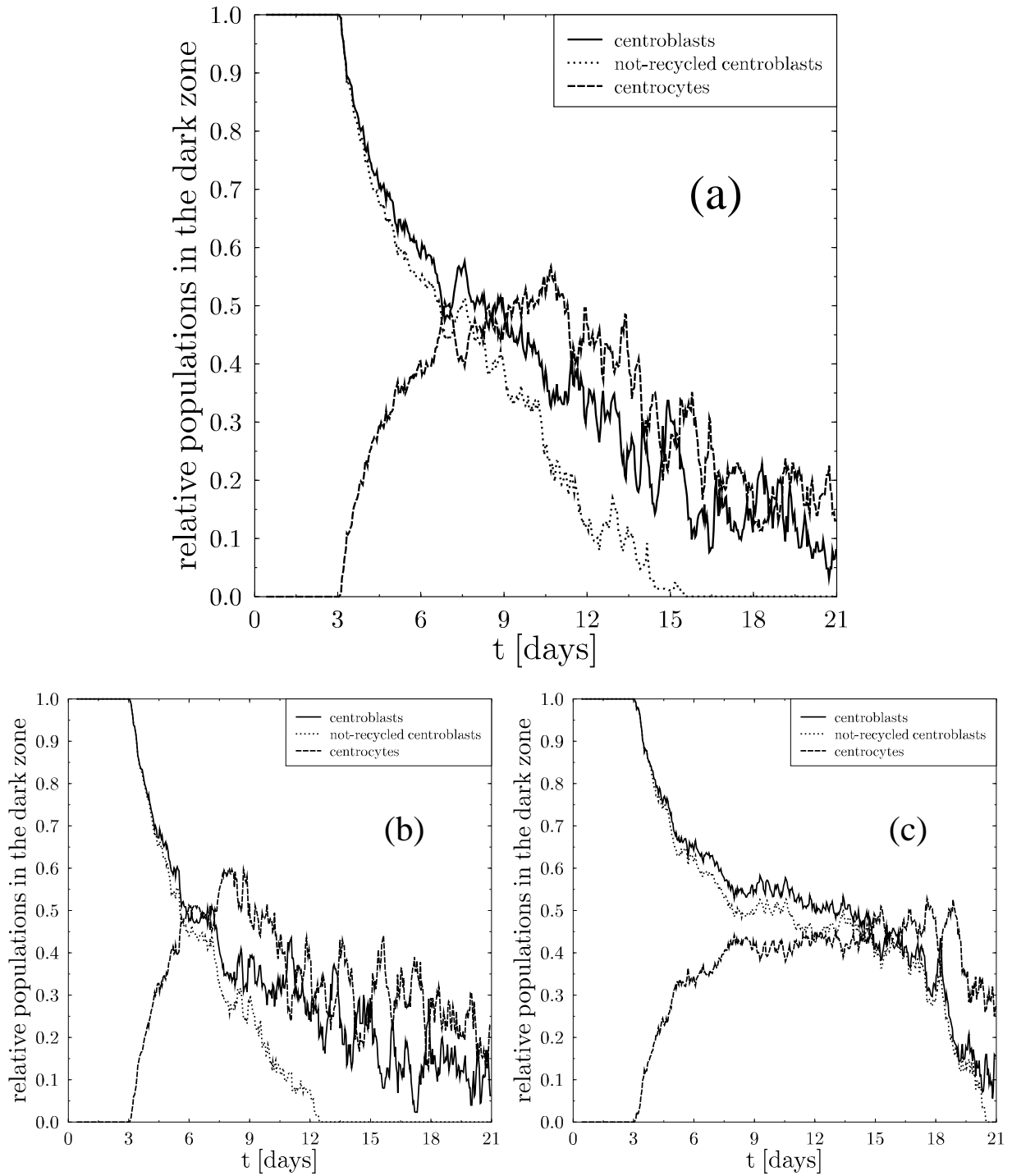


Figure 5: Representative time courses of the relative centroblast and centrocyte populations in the lower hemisphere of the GC for different durations of the dark zone. In (a) the parameters in Tab. 1 were used. The production rate of signal molecules has been changed to $s = 6/hr$ (and the apoptosis rate to $z = 1/8 hr$) in (b) and to $s = 12/hr$ in (c). The dark zone breaks down after 8.3 days (a), 6.9 days (b), 14.9 days (c). Recycled B-cells have practically no impact on the dark zone population.

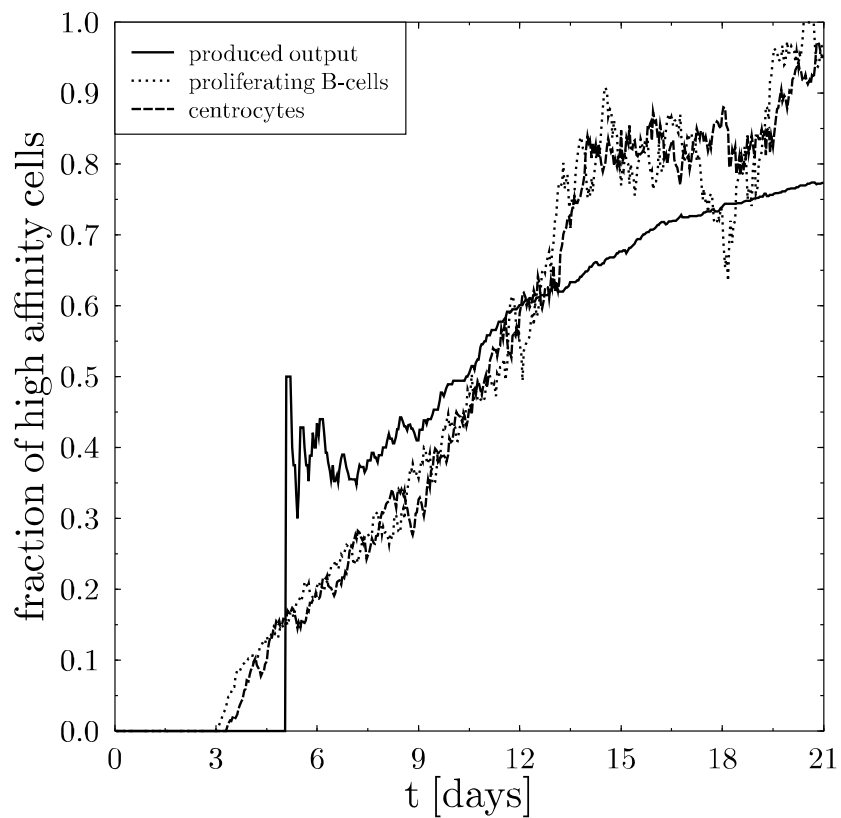


Figure 6: The time course of the fraction of high affinity cells (cells which bind with a probability of at least 30%) in the GC reaction is shown for centroblasts, centrocytes, and for the sum of all output cells produced during the whole GC reaction. The parameters in Tab. 1 were used.

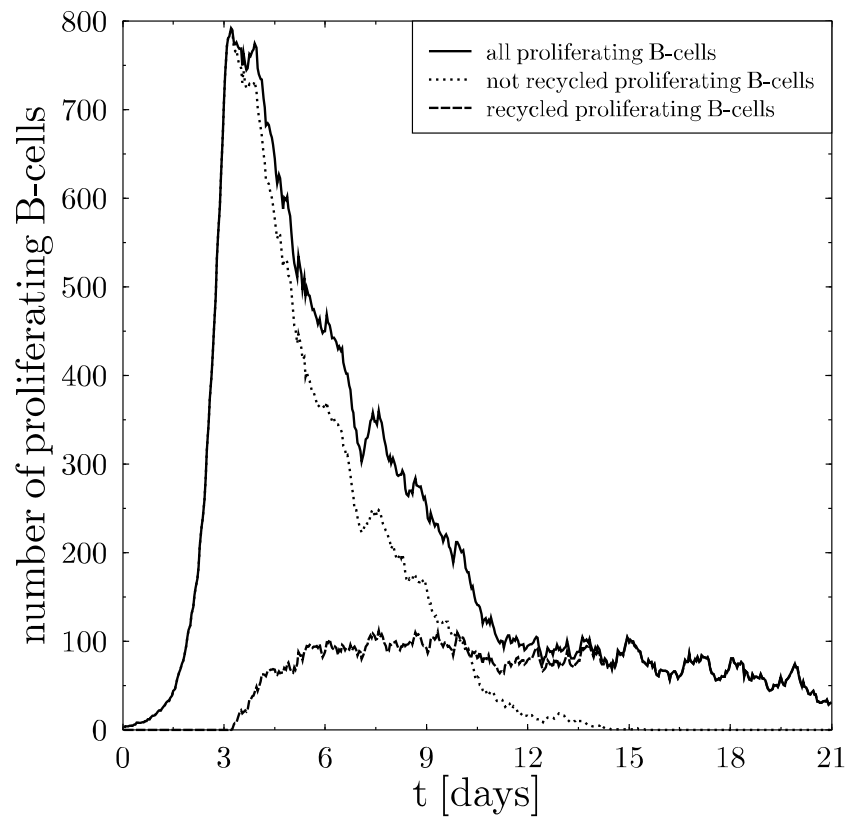


Figure 7: The time course of the whole population of centroblasts, the subset of recycled centroblasts, and non-recycled centroblasts in the GC reaction. The parameters in Tab. 1 were used.

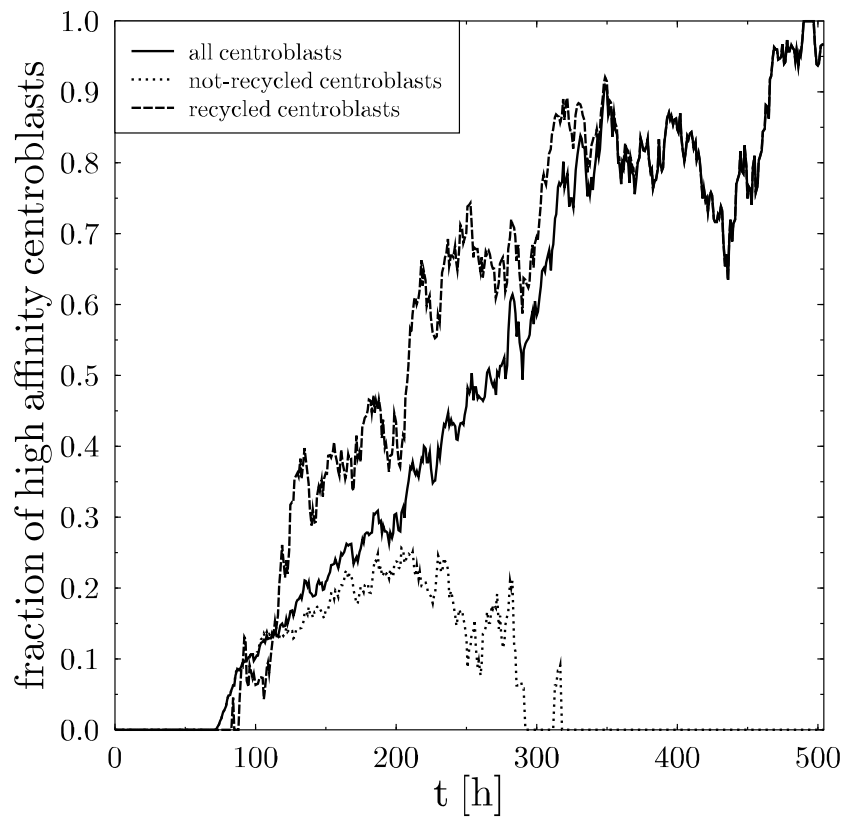


Figure 8: The time course of the fraction of high affinity centroblasts in the GC reaction (cells which bind to FDCs with a probability of at least 30%) shown for the total centroblast population and for the subsets of recycled B-cells and non-recycled centroblasts separately. The fractions are defined with respect to the total population of the corresponding subset (e.g. high affinity recycled B-cells divided by all recycled B-cells). The parameters in Tab. 1 were used.

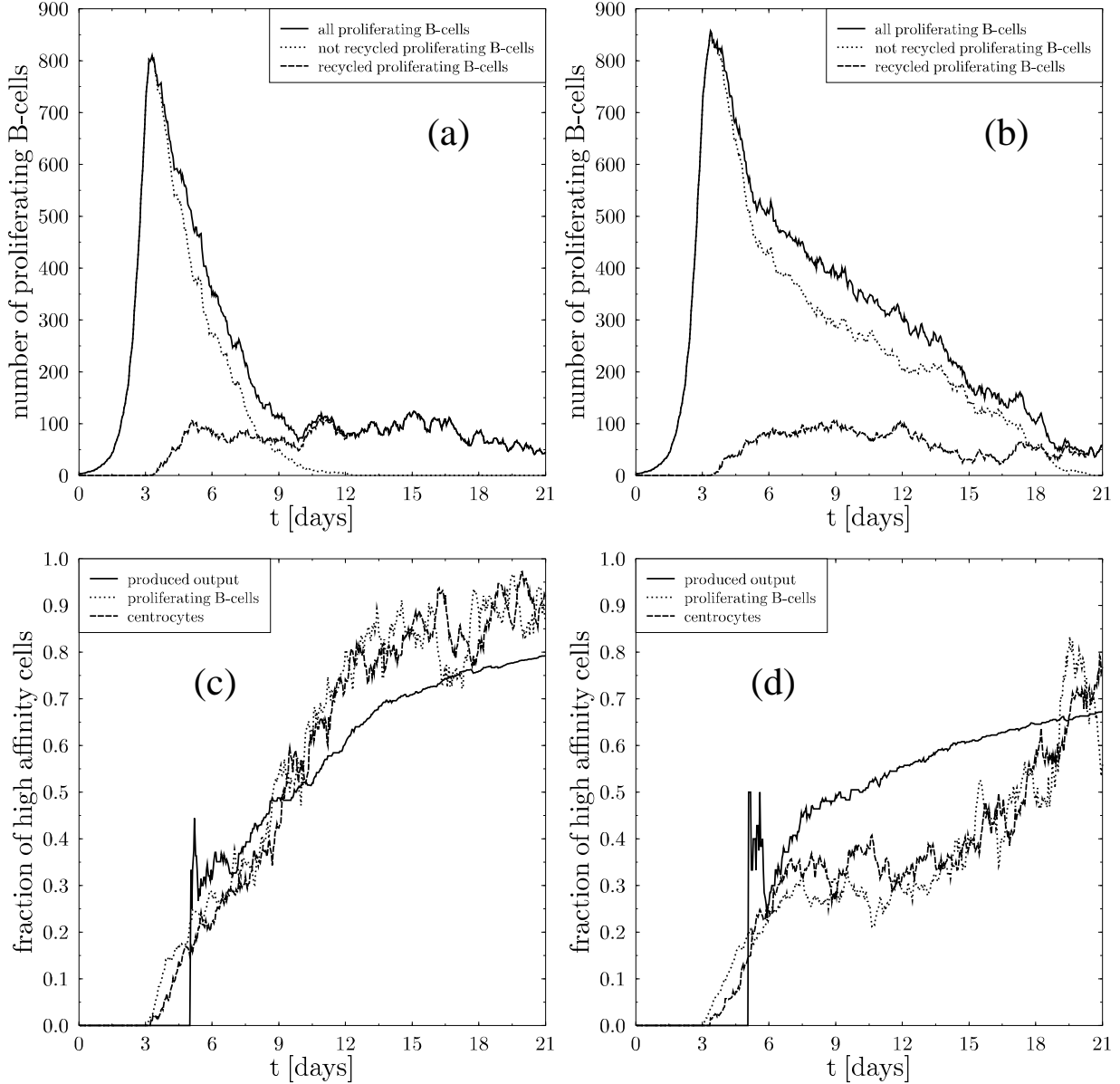


Figure 9: The time courses of the populations of non-recycled centroblasts, recycled centroblasts, and the sum of all proliferating B-cells, as well as of the fractions of high affinity B-cells. The duration of the dark zone was changed with respect to Fig. 6 and 7 by the use of different differentiation signal productions rates of $s = 12/hr$ in (a,c) and $s = 6/hr$ in (b,d). The apoptosis rate is $z = 1/(8 hr)$ in (b,d). All other parameters are like in Tab. 1. One observes a clear correlation between the moment of domination of recycled B-cells (see (a) and (b)) and the starting time of a phase of step increase in the affinity (see (c) and (d)).

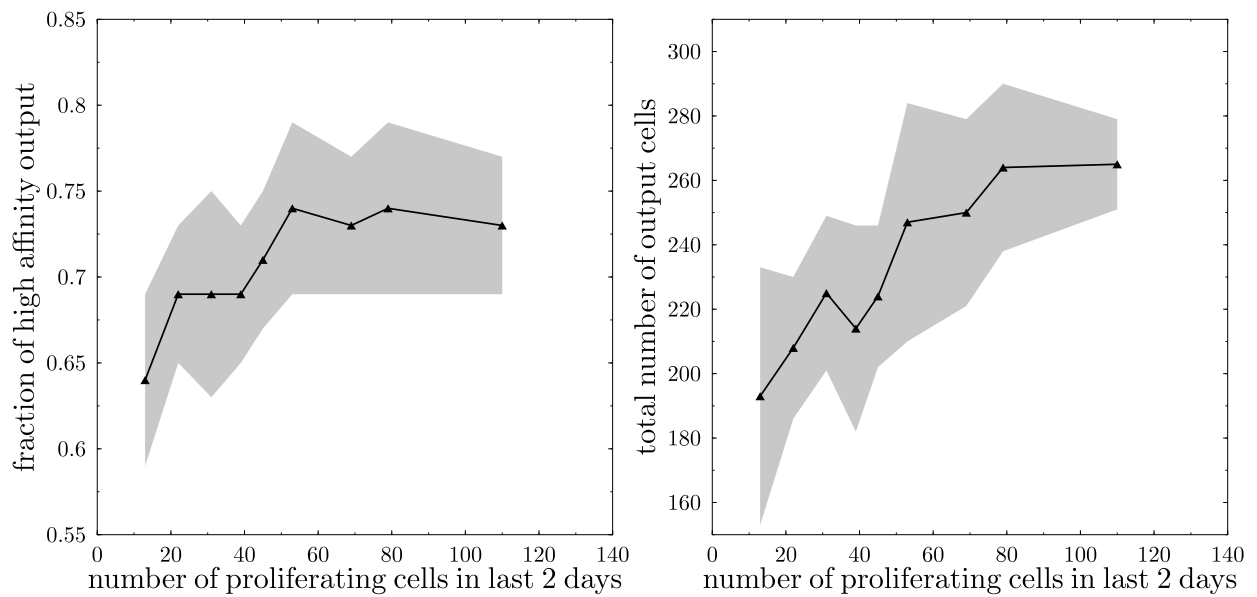


Figure 10: The dependence of the fraction of high affinity output cells and of the total number of produced output cells (summed up to the end of the GC reaction) on the number of proliferating cells that remain in average in the GC during the last 2 days of the reaction. The grey area denotes one standard deviation of the average values along the full line. The parameters in Tab. 1 were used with different rates of centroblast differentiation signal production s , i.e. with dark zones of variable duration. The centroblast differentiation rate g_1 is adapted correspondingly.

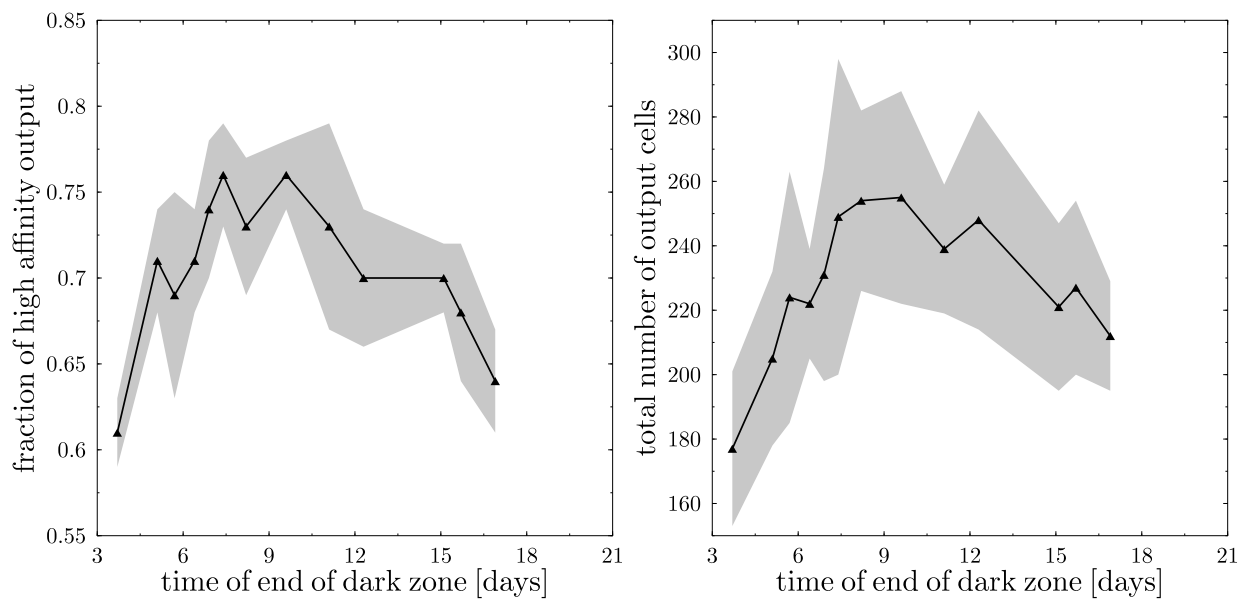


Figure 11: The dependence of the fraction of high affinity output cells and of the total number of produced output cells (summed up to the end of the GC reaction) on the duration of the dark zone. The grey area denotes one standard deviation of the average values along the full line. The parameters in Tab. 1 were used, where the production rate of the centroblast differentiation signal s and the centroblast differentiation rate g_1 were varied in order to generate different durations of the dark zone.

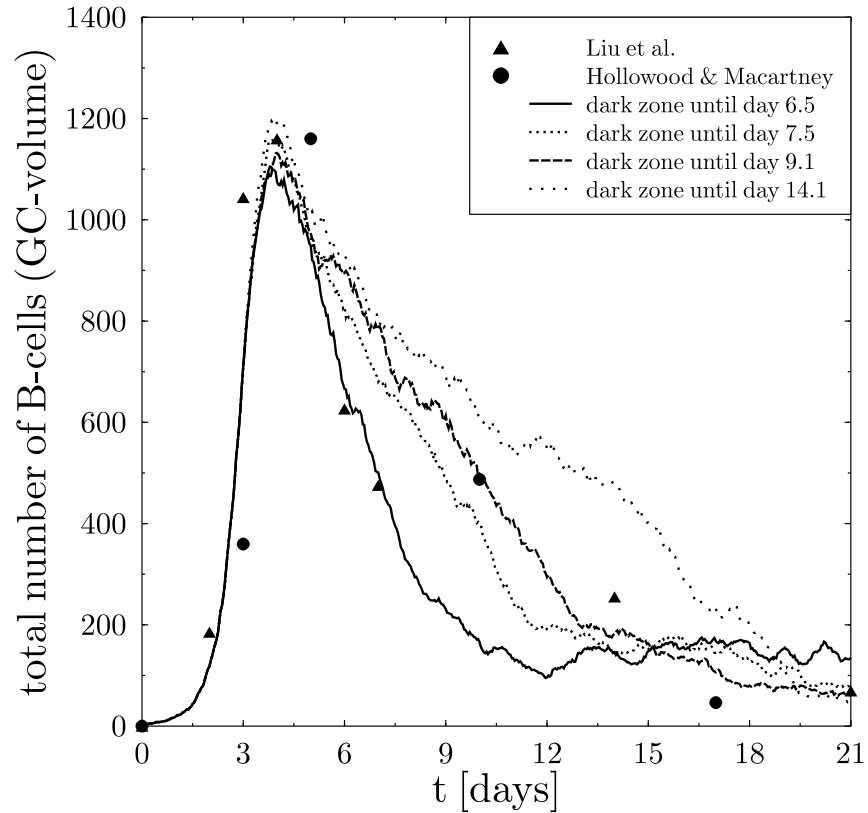


Figure 12: Representative time courses of the total number of B-cells (i.e. centroblasts and centrocytes) in the GC reaction for four different durations of the dark zone. The parameters in Tab. 1 were used for the GC reactions with dark zones until day 7.5 and 9.1. The short dark zone was generated with a faster differentiation signal production of $s = 12/hr$. In the case of the long dark zone the centroblast differentiation signal is produced with a lower rate of $s = 6/hr$ and the centroblast differentiation rate is $g_1 = 1/(5.65 hr)$. For comparison, the average data from (Liu *et al.*, 1991; Hollowood & Macartney, 1992) were normalized to the maximum of the simulation results and rescaled correspondingly.